Higher Nuclearity Fe,Ru Mixed-Metal Dicarbide Cluster Compounds Derived from Ethynediyldiiron Complex $(\eta^5\text{-}C_5Me_5)(CO)_2Fe-C\equiv C-Fe(\eta^5\text{-}C_5Me_5)(CO)_2$

Munetaka Akita,* Shuichiro Sugimoto, Hideki Hirakawa, Shin-ichi Kato, Masako Terada, Masako Tanaka, and Yoshihiko Moro-oka

Chemical Resources Laboratory, Tokyo Institute of Technology, 4259 Nagatsuta, Midori-ku, Yokohama 226-8503, Japan

Received November 27, 2000

Reaction of the ethynyliron complexes FP−C≡C−H [FP = Fp (**1**), Fp* (**1***); Fp = (η^5-C_5H_5)-$Fe(CO)_2$; Fp* = (η^5-C_5Me_5)$Fe(CO)_2$] with $Ru_3(CO)_{12}$ in refluxing benzene affords triruthenium μ-η^1(Ru1):η^2(Ru2):η^2(Ru3)-acetylide cluster type compounds $Ru_3(CO)_9[\mu_3\text{-}\eta^1\text{:}\eta^2\text{:}\eta^2\text{-}C\equiv C-FP]$ [FP = Fp (**3**), Fp* (**3***)] in a manner similar to the reaction of 1-alkynes. In contrast to the clean reaction of **1** and **1***, reaction of the ethynediyldiiron complex, Fp*−C≡C−Fp* (**2***), gives a complicated mixture of products, from which $Cp^*_2Fe_2Ru_2(\mu_4\text{-}C_2)(CO)_{10}$ (**5***) and $Cp^*_2Fe_2Ru_6(\mu_6\text{-}C_2)(CO)_{17}$ (**6***) are isolated and characterized as *permetalated ethene* and *permetalated ethane*, respectively, by X-ray crystallography. It is revealed that the permetalated hydrocarbon structures in **5*** and **6*** are constructed via formal addition of a dimetallic species to the C−C triple bond in **2***. The octanuclear complexes **6*** and **6** (Cp derivative) are also prepared by thermal dimerization of the tetranuclear $FeRu_3(\mu\text{-}C_2)$ core in **3*** and **3**. Higher nuclearity cluster compounds including the heptanuclear dicarbide cluster compound $CpFeRu_6(\mu_5\text{-}C_2)(\mu_5\text{-}C_2H)(CO)_{16}$ (**12**) and the heptanuclear bis(dicarbide) cluster compound $Cp_2Fe_2Ru_5(\mu_5\text{-}C_2)_2(CO)_{17}$ (**15**) are obtained not only by thermolysis but also by one-electron oxidation of the deprotonated anionic form of **3** (**13**).

Introduction

The C≡C functional group can bind metal centers together to form polynuclear compounds. In particular, transition metal acetylide complexes turn out to be versatile starting compounds for cluster compounds because the metal center originally σ-bonded to the acetylide ligand may take part in bond formation with the added metal species to form a three-dimensional metal framework.[1] The resulting structures have been recognized as models for surface-bound hydrocarbyl species,[2] which occur during conversions of syngas and hydrocarbon effected by heterogeneous catalysts.[3] Previous studies have revealed a variety of coordination modes of acetylide cluster compounds, but many of them contain acetylide substituents, which may not be always suitable as surface species (e.g., ester). In this regard, ethynyl (M−C≡C−H) and ethynediyl complexes (M−C≡C−M)[4] containing the substituents of the simple composition are expected to display structural and reaction features closer to those of the actual surface-bound species. A polynuclear complex with the C_2 ligand can be recognized as a dicarbide cluster compound, which is a member of transition metal complexes associated with carbon allotropes (C_x) including monocarbon species and fullurenes.[5,6] We have been carrying out a synthetic study of polynuclear C2[7] complexes derived from the ethynyl [FP−C≡C−H: FP = Fp (**1**), Fp* (**1***); Fp = (η^5-C_5H_5)$Fe(CO)_2$; Fp* = (η^5-C_5Me_5)$Fe(CO)_2$] and ethynediyl iron complexes [Fp*−C≡C−Fp* (**2***)] (Scheme

(1) (a) Sappa, E.; Tiripicchio, A.; Braunstein, P. *Chem. Rev.* **1983**, *83*, 203. (b) Sappa, E.; Tiripicchio, A.; Carty, A. J.; Toogood, G. E. *Prog. Inorg. Chem.* **1987**, *35*, 437. (c) Raithby, P. R.; Rosales, M. J. *Adv. Inorg. Chem. Radiochem.* **1985**, *29*, 169. (d) Carty, A. J. *Pure Appl. Chem.* **1982**, *54*, 113. (e) *Comprehensive Organometallic Chemistry II*; Abel, E. W., Stone, F. G. A., Wilkinson, G., Eds.; Pergamon: Oxford, 1995; Vol. 7, Chapter 4.

(2) (a) Silvestre, J.; Hoffmann, R. *Langmuir* **1985**, *1*, 621. (b) Masters, C. *Adv. Organomet. Chem.* **1979**, *19*, 63. (c) Muetterties, E. L.; Rhodin, T. N.; Band, E.; Brucker, C. F.; Pretzer, W. R. *Chem. Rev.* **1979**, *79*, 79. (d) Roofer-DePoorter, C. K. *Chem. Rev.* **1981**, *81*, 447. (e) Herrmann, W. A. *Angew. Chem., Int. Ed. Engl.* **1982**, *21*, 117. (f) Cutler, A. R.; Hanna, P. K.; Vites, J. C. *Chem. Rev.* **1988**, *88*, 1363 and references cited therein. For carbide complexes: (g) Tachikawa, M.; Muetterties, E. L. *Prog. Inorg. Chem.* **1981**, *28*, 203. (h) Bradley, J. S. *Adv. Organomet. Chem.* **1983**, *22*, 1. (i) Shriver, D. F.; Sailor, M. J. *Acc. Chem. Res.* **1988**, *21*, 374.

(3) (a) Somorjai. G. A. *Introduction to Surface Science Chemistry and Catalysis*; Wiley-Interscience: New York, 1994. (b) Ertl, G.; Knözinger, H.; Weitkamp, J. *Handbook of Heterogeneous Catalysis*; VCH: Weinheim, 1997.

(4) (a) Appel, M.; Heidrich, J.; Beck, W. *Chem. Ber.* **1987**, *120*, 1087. (b) Heidrich, J.; Steimann, M.; Appel, M.; Beck, W.; Phillips, J. R.; Trogler, W. C. *Organometallics* **1990**, *9*, 1296. (c) Ogawa, H.; Onitsuka, K.; Joh, T.; Takahashi, S. *Organometallics* **1988**, *7*, 2257. (d) Kousantonis, G. A.; Selegue, J. P. *J. Am. Chem. Soc.* **1991**, *113*, 2316. (e) St. Clair, M.; Schaefer, W. P.; Bercaw, J. E. *Organometallics* **1991**, *10*, 525. (f) Lemke, F. R.; Szalda, D. J.; Bullock, R. M. *J. Am. Chem. Soc.* **1991**, *113*, 8466. (g) Chan, M. C.; Tsai, Y. J.; Chen, C. T.; Lin, Y. C.; Tseng, T. W.; Lee, G. H.; Wang, Y. *Organometallics* **1991**, *10*, 378. (h) Yang, Y.-L.; Wang, L. J.-J.; Huang, S.-L.; Chen, M.-C.; Lee, G.-H.; Wang, Y. *Organometallics* **1997**, *16*, 1573. See also reference cited in refs 8a and 8k.

(5) (a) Allegra, G.; Peronaci, E. M.; Ercoli, R. *J. Chem. Soc., Chem. Commun.* **1966**, 549. (b) Brice, M. D.; Penfold, B. R. *Inorg. Chem.* **1972**, *11*, 1381. (c) Jensen, M. P.; Philipps, D. A.; Sabat, M.; Shriver, D. F. *Organometallics* **1992**, *11*, 1859. (d) Jensen, M. P.; Sabat, M.; Shriver, D. F. *J. Cluster. Sci.* **1990**, *1*, 75. (e) Gervasio, G.; Rosetti, R.; Bor, G. *Inorg. Chem.* **1984**, *23*, 2073. (f) Bruce, M. I. *Coord. Chem. Rev.* **1997**, *166*, 91. (g) Bruce, M. I. *J. Cluster Sci.* **1997**, *8*, 293. (h) Adams, C. J.; Bruce, M. I.; Skelton, B. W.; White, A. H. *J. Chem. Soc., Chem. Commun.* **1992**, 26. (i) See references cited in refs 5g and 5h.

10.1021/om001009c CCC: $20.00
Publication on Web 03/17/2001

Scheme 1

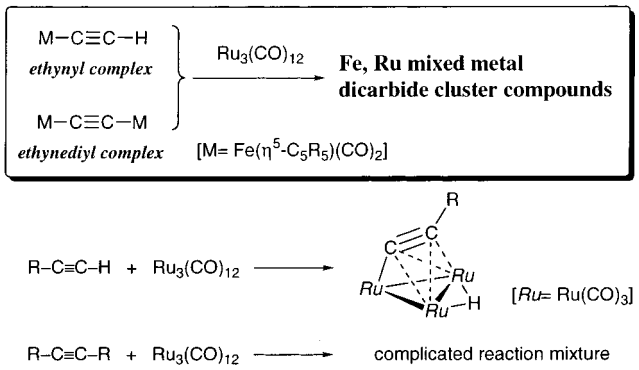

1),[7,8b,k] and have reported various novel aspects of these systems including H shift on the C_2 bridge, conversion to C_2H_x species, and reversible M−M bond scission.[8]

Herein we disclose details of the results of interaction of the C2 iron complexes (**1**, **1***, and **2***)[7] with $Ru_3(CO)_{12}$, leading to higher nuclearity Fe,Ru mixed-metal dicarbide cluster compounds. Preliminary reports already appeared,[8c,h] and studies on the molecular orbital analysis of polynuclear C_2 complexes including the compounds presented herein and related compounds were reported recently by Halet et al.[9]

Reaction of alkynes with $Ru_3(CO)_{12}$ has long been studied extensively (Scheme 1). Previous studies reveal that reaction with 1-alkynes produces the triruthenium acetylide cluster compounds in a selective manner via C−H bond oxidative addition, whereas internal alkynes afford various products depending on the structure of the alkyne substituents and the reaction conditions.[10]

Results and Discussion

Interaction of Ethynyliron Complexes FP−C≡C−H [FP = Fp (1), Fp* (1*)] with $Ru_3(CO)_{12}$, Leading to Acetylide Cluster Type Tetranuclear Dicarbide Cluster Compounds (μ_3-C≡C−FP)(μ-H)-$Ru_3(CO)_9$ [FP = Fp (3), Fp* (3*)]. Treatment of the ethynyl complexes **1** and **1*** with $Ru_3(CO)_{12}$ in refluxing benzene gave yellow-orange crystals **3** and **3***, respectively, as sole organometallic products (eq 1). The simple

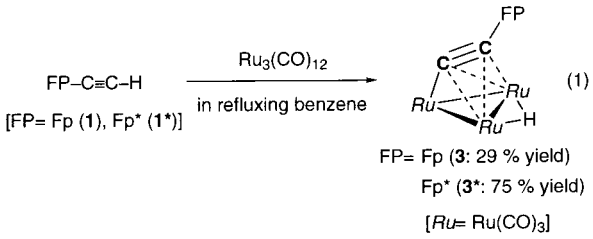

^{1}H NMR spectra containing the characteristic shielded hydride signals [δ_H −20.05 (**3**), −19.56 (**3***)] in addition to the η^5-C_5R_5 resonances [δ_H 3.90 (**3**), 1.25 (**3***)] indicated formation of the acetylide cluster type products analogous to the reaction product of 1-alkyne (Scheme 1).

The cluster compound **3** was characterized by X-ray crystallography, and the molecular structure and selected structural parameters are shown in Figure 1 and Table 1, respectively. Because no bonding interaction is present between the distal Fe center and the Ru_3 triangle, the Fp group simply works as an acetylide substituent. In other words, **3** is better described as a triruthenium μ-η^1(Ru1):η^2(Ru2):η^2(Ru3)-acetylide cluster compound with the Fp−C≡C acetylide ligand rather than as a tetranuclear μ-η^1(Fe):η^1(Ru1):η^2(Ru2):η^2(Ru3)-dicarbide cluster compound. The core structure of **3** is very similar to that in the previously reported organic

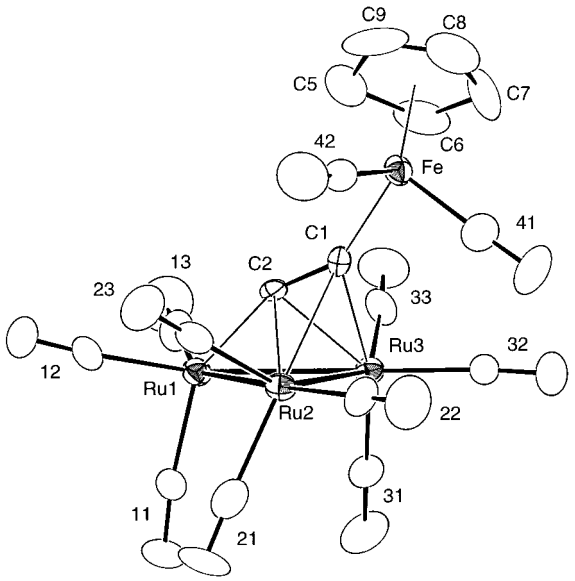

Figure 1. Molecular structure of **3** drawn (with displacement ellipsoid amplitudes) at the 30% probability level. Labels without atom names are for CO ligands.

(6) (a) Beck, W.; Niemer, B.; Wieser, M. *Angew. Chem., Int. Ed. Engl.* **1993**, *32*, 923. (b) Lang, H. *Angew. Chem., Int. Ed. Engl.* **1994**, *33*, 547. (c) Bunz, U. H. F. *Angew. Chem., Int. Ed. Engl.* **1996**, *35*, 969. (d) Altman, M.; Bunz, U. H. F. *Angew. Chem., Int. Ed. Engl.* **1995**, *34*, 569. (e) Bruce, M. I. *Chem. Rev.* **1998**, *98*, 2797. (f) Balch, A. L.; Olmstead, M. M. *Chem. Rev.* **1998**, *98*, 2133. (g) Paul, F.; Meyer, W. E.; Toupet, L.; Jiao, H.; Gladysz, J. A.; Lapinte, C. *J. Am. Chem. Soc.* **2000**, *122*, 9405. (h) Dembinski, R.; Bartik, T.; Bartik, B.; Jaeger, M.; Gladysz, J. A. *J. Am. Chem. Soc.* **2000**, *122*, 810.

(7) The term "C2" stands for two carbon systems including C_2 and C_2H species. All Cp* complexes are indicated by asterisks in their compound numbers. Fp: (η^5-C_5H_5)Fe(CO)$_2$. Fp*: (η^5-C_5Me_5)Fe(CO)$_2$. Cp: η^5-C_5H_5. Cp*: η^5-C_5Me_5. *Ru*: Ru(CO)$_3$. **Ru**: Ru(CO)$_2$.

(8) C_2 complexes: (a) Akita, M.; Moro-oka, Y. *Bull. Chem. Soc. Jpn.* **1995**, *68*, 420. (b) Akita, M.; Oyama, S.; Terada, M.; Moro-oka, Y. *Organometallics* **1990**, *9*, 816. (c) Akita, M.; Sugimoto, S.; Tanaka, M.; Moro-oka, Y. *J. Am. Chem. Soc.* **1992**, *114*, 7581. (d) Akita, M.; Ishii, N.; Takabuchi, A.; Tanaka, M.; Moro-oka, Y. *Organometallics* **1994**, *13*, 258. (e) Akita, M.; Takabuchi, A.; Terada, M.; Ishii, N.; Tanaka, M.; Moro-oka, Y. *Organometallics* **1994**, *13*, 2516. (f) Akita, M.; Terada, M.; Ishii, N.; Hirakawa, H.; Moro-oka, Y. *J. Organomet. Chem.* **1994**, *473*, 175. (g) Akita, M.; Hirakawa, H.; Moro-oka, Y. *Organometallics* **1995**, *14*, 2775. (h) Akita, M.; Hirakawa, H.; Tanaka, M.; Moro-oka, Y. *J. Organomet. Chem.* **1995**, *485*, C14. C_1 complexes: (i) Takahashi, Y.; Akita, M.; Moro-oka, Y. *J. Chem. Soc., Chem. Commun.* **1997**, 1557. Allenylidene complexes: (j) Akita, M.; Kato, S.-I.; Terada, M.; Masaki, Y.; Tanaka, M.; Moro-oka, Y. *Organometallics* **1997**, *16*, 2392. C_n complexes ($n \geq 4$): (k) Akita, M.; Chung, M.-C.; Sakurai, A.; Sugimoto, S.; Terada, M.; Tanaka, M.; Moro-oka, Y. *Organometallics* **1997**, *16*, 4882. (l) Akita, M.; Chung, M.-C.; Terada, M.; Miyauti, M.; Tanaka, M.; Moro-oka, Y. *J. Organomet. Chem.* **1998**, *565*, 49. (m) Akita, M.; Sakurai, A.; Moro-oka, Y. *J. Chem. Soc., Chem. Commun.* **1999**, 101. (n) Sakurai, A.; Akita, M.; Moro-oka, Y. *Organometallics* **1999**, *18*, 3241. (o) Chung, M.-C.; Sakurai, A.; Akita, M.; Moro-oka, Y. *Organometallics* **1999**, *18*, 4684. (p) Akita, M.; Chung, M.-C.; Sakurai, A.; Moro-oka, Y. *J. Chem. Soc., Chem. Commun.* **2000**, 1285.

(9) (a) Frapper, G.; Halet, J.-F.; Bruce, M. I. *Organometallics* **1995**, *14*, 5044. (b) Frapper, G.; Halet, J.-F.; Bruce, M. I. *Organometallics* **1997**, *16*, 2590.

(10) (a) *Comprehensive Organometallic Chemistry*; Wilkinson, G., Abel, E. W., Stone, F. G. A., Eds.; Pergamon: Oxford, 1982; Vol. 4, Chapter 32.5. (b) *Comprehensive Organometallic Chemistry II*; Abel, E. W., Stone, F. G. A., Wilkinson, G., Eds.; Pergamon: Oxford, 1995; Vol. 7, Chapter 13.

Table 1. Comparison of Structural Parameters for Acetylide Cluster Type Compounds

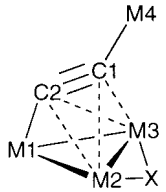

	3 M1, M2 = Ru, Ru M3, M4 = Ru, Fe X = H	**10*** M1, M2 = Fe, Ru M3, M4 = Ru, Fe X = H	**13** M1, M2 = Ru, Ru M3, M4 = Ru, Fe X = none	**4**[a] M1, M2 = Ru, Ru M3, M4 = Ru, Bu^t X = H	**14**[b] M1, M2 = Ru, Ru M3, M4 = Ru, Bu^t none	**16**[c] M1, M2 = Fe, Fe M3, M4 = Fe, Fe none
			Bond Lengths (Å)			
C1−C2	1.33(2)	1.32(1)	1.271(9)	1.315(3)	1.27(3)	1.288(5)
C1−M4	1.90(1)	1.947(9)	1.984(8)	1.500(3)	1.54(3)	1.959(3)
C1−M2	2.41(1)	2.395(8)	2.347(7)	2.268(3)	2.24(2)	2.190(3)
C1−M3	2.40(1)	2.377(8)	2.349(7)	2.271(3)	2.24(2)	2.212(3)
C2−M1	2.01(1)	1.834(9)	1.984(8)	1.947(3)	1.95(2)	1.839(3)
C2−M2	2.22(1)	2.203(8)	2.189(7)	2.207(3)	2.18(2)	2.020(3)
C2−M3	2.20(1)	2.169(8)	2.199(7)	2.214(3)	2.16(2)	2.021(3)
M1−M2	2.781(2)	2.707(2)	2.7891(9)	2.795(3)	2.800(3)	2.6207(7)
M1−M3	2.774(2)	2.699(1)	2.793(1)	2.799(3)	2.790(3)	2.6252(8)
M2−M3	2.819(2)	2.791(1)	2.6886(9)	2.792(3)	2.665(3)	2.5048(8)
M1−CO	1.89−1.94(2)	1.80−1.86(1)	1.87−1.90(1)	1.898−1.931(4)	1.90−1.92(2)	1.765−1.784(4)
M2−CO	1.96−2.00(2)	1.92−1.94(1)	1.861−1.890(9)	1.910−1.938(4)	1.88−1.89(2)	1.762−1.784(4)
M3−CO	1.90(2)	1.93−1.96(1)	1.86−1.88 (1)	1.910−1.944(4)	1.85−1.92(2)	1.772−1.780(4)
M4−CO	1.80(2)	1.76−1.78(1)	1.744−1.768(9)			1.768−1.772(4)
			Bond Angles (deg)			
C2−C1−M4	149(1)	147.7(7)	149.3(6)	141.0(2)	141(2)	147.3(3)
C2−C1−M2	65.5(7)	65.5(5)	67.0(4)	70.4(1)	76(1)	*d*
C2−C1−M3	65.3(8)	64.6(5)	67.4(5)	70.6(1)	77(1)	*d*
M2−C1−M3	71.7(4)	71.6(2)	69.9(2)	75.9(1)	73(1)	*d*
M4−C1−M2	135.3(7)	138.9(4)	136.0(3)	135.2(2)	134(1)	*d*
M4−C1−M3	135.9(7)	134.2(4)	133.1(4)	135.0(2)	138(1)	*d*
C1−C2−M1	159(1)	161.4(7)	160.1(6)	153.7(2)	156(1)	161.6(3)
M2−C2−M3	79.2(4)	79.3(3)	75.6(2)	78.3(1)	76(1)	*d*
C1−C2−M2	81.6(8)	81.5(5)	80.7(5)	75.5(1)	76(1)	*d*
C1−C2−M3	81.6(8)	82.0(5)	80.4(5)	75.3(1)	77(1)	*d*
M1−C2−M2	82.2(4)	83.7(3)	83.8(3)	84.3(1)	85(1)	*d*
M1−C2−M3	82.3(4)	84.3(3)	83.7(3)	84.3(1)	85(1)	*d*
M2−M1−M3	61.00(4)	62.16(4)	57.58(2)	59.9(1)	56.9(1)	57.04(2)
M1−M2−M3	59.38(4)	58.77(3)	61.29(2)	60.1(1)	61.3(1)	61.57(2)
M1−M3−M2	59.62(4)	59.07(4)	61.13(2)	60.0(1)	61.7(1)	61.39(2)
M1−C−O	173−177(2)	178−180(1)	176.9−179.7(8)	176.9−178.3(1)	174−177(2)	178.3−179.4(4)
M2−C−O	176−177(2)	174−179(2)	176.2−177.2(8)	176.0−179.0(1)	175−178(2)	176.6−178.3(3)
M3−C−O	176−180(1)	176−179(1)	177−178(1)	175.0−179.9(3)	175−178(2)	176.4−177.5(4)
M4−C−O	178(2)	176(1)	175.5−177.9(8)			172.9−178.0(4)

[a] $Ru_3(\mu_3\text{-}C{\equiv}C{-}Bu^t)(\mu\text{-}H)(CO)_9$, neutron diffraction, ref 11. [b] $(AsPh_4)[Ru_3(\mu_3\text{-}C{\equiv}C{-}Bu^t)(CO)_9]$, ref 21. [c] A tetrairon analogue of **13**, $(PPN)[Fe_3(\mu_3\text{-}C{\equiv}C{-}Fp)(CO)_9]$, ref 5d. [d] Not reported.

acetylide cluster compound $(\mu_3\text{-}C{\equiv}C{-}Bu^t)(\mu\text{-}H)Ru_3(CO)_9$ (**4**) [R = Bu^t (Scheme 1); Table 1].[11] Upon coordination, the C−C distance [1.33(2) Å] is slightly elongated compared to that of the starting compound [**1***: 1.173-(4) Å].[8k] The Fe−C1 [1.90(1) Å] and Ru1−C2 distances [2.01(1) Å] fall in the range of single bond lengths, and the similar distances between the other two Ru centers and the acetylide carbon atoms [Ru2−C1 2.41(1) Å, Ru3−C1 2.40(1) Å; Ru2−C2 2.22(1) Å, Ru3−C2 2.20(1) Å] typical for π coordination indicate symmetrical coordination of the C2−C1−Fe linkage with respect to the Ru_3 triangle. Although the hydride atom cannot be located, it should be on the Ru2−Ru3 bond, the distance [2.819(2) Å] of which is slightly longer than the other two Ru−Ru distances [2.774(2) and 2.781(2) Å]. In accord with the structure, the C_2 signals [δ_C 79.7, 174.1 (**3**); δ_C 96.8, 168.1 (**3***)] appear in the range analogous to that for trinuclear acetylide cluster compounds of $(\mu_3\text{-}C{\equiv}C{-}R)M_3$ type,[1] and the deshielded signals are assigned to C2. Details of the structural aspects will be discussed later as compared with related compounds.

Interaction of Ethynediyl Complex Fp*−C≡C−Fp* (2*) with $Ru_3(CO)_{12}$. Sequential Formation of Permetalated Ethene (5*) and Ethane Type Cluster Compounds (6*). In contrast to the clean reaction of **1** and **1***, reaction of **2*** gave a complicated mixture of products in a manner similar to the reaction of internal alkynes (Scheme 1).[10] In addition to the two known compounds (**3*** and Fp^*_2), two new compounds **5*** and **6*** showing only one Cp* resonance (^{1}H NMR) were isolated from the reaction mixture and characterized as *permetalated ethene* and *permetalated ethane*, respectively, by X-ray crystallography (Scheme 2). Molecular structures of **5*** and **6*** together with expanded views of the core parts are shown in Figures 2 and 3, and selected structural parameters are listed in Tables 2 and 3.

Complex **5*** is found to be a tetranuclear Fe_2Ru_2 complex containing one C_2 ligand and has a C_2-symmetrical structure with respect to the axis passing

(11) Sappa, E.; Gambino, O.; Milone, L.; Cetini, G. *J. Organomet. Chem.* **1972**, *39*, 169.

Scheme 2

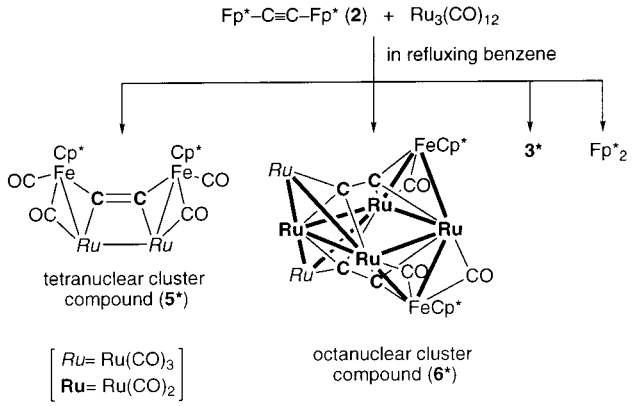

through the midpoints of the C−C and Ru−Ru bonds. The four metal atoms are linked by metal−metal bonds to form an open-rectangular array, which is slightly twisted as can be seen from a top view of the core structure (Figure 3c; Fe−Ru−Ru*−Fe* dihedral angle is 24°). The C_2 ligand interacts with the metal array through σ bonds [Fe−C1, 1.946(7) Å; Ru−C1, 2.204(7)], although the Ru−C1 distance is in the upper limit of Ru−C σ bond lengths and comparable to π bond lengths [cf. σ bond, 2.026(7) and 2.033(7) Å for $Cp_2Ru_2(\mu$-$C{=}CH_2)(CO)_3$;[12] π bond, see, for example, the Ru2,3−C12 lengths (2.2−2.4 Å) for **3** (Table 1)]. The C1−C1* distance [1.24(1) Å] is longer than the C≡C distance of the ethynediyl complex **2**# [η^5-C_5Me_4Et derivative of **2***] (with two independent molecules): 1.206(6), 1.211(6) Å][8k] but substantially shorter than normal $C(sp^2){=}C(sp^2)$ lengths (1.34 Å).[13] The C−C linkage, which spans the two iron atoms at both the ends of the open-rectangular array, causes distortion of the $Fe_2Ru_2(\mu_4$-$C_2)$ moiety as judged by the slightly elongated Ru1−Ru1* distance [2.963(2) Å; cf. Ru−Ru lengths (∼2.8 Å) in Table 1] and the twisting of the Fe_2Ru_2 array. The two Cp* rings are located in trans configuration with respect to the $Fe_2Ru_2(\mu_4$-$C_2)$ moiety to avoid steric repulsion between them. NMR data suggesting a symmetrical structure are consistent with the C_2-symmetrical X-ray structure. The C_2 signal at δ_C 177.2, assigned by comparison with a sample obtained from ^{13}CO-enriched $Ru_3(CO)_{12}$, is highly shielded compared to the α-carbon signals (δ_C ∼300) of dinuclear μ-vinylidene complexes [$M_2(\mu$-$C_\alpha{=}CR_2)$],[6d] which can be regarded as a partial structure of **5***. Because the five carbonyl ligands are observed separately, they do not exchange at ambient temperature in a solution. Although a number of related complexes including μ-vinylidene complexes[6d] and alkyne cluster complexes[1] have been reported so far, complex **5*** is the first example of *a permetalated ethene*, $(Cp^*Fe)_2Ru_2(\mu_4$-$C{=}C)(\mu$-$CO)_2(CO)_8$. The EHMO calculation done by Halet on the CpRu analogue $(CpRu)_2Ru_2(\mu_4$-$C{=}C)(\mu$-$CO)_2(CO)_8$ clearly indicates that it is a permetalated ethene in which the filled out-of-plane π-type p orbitals of the C_2 unit play a minor role in the M−C bonding.[9a] The p orbitals form a π bond as found in ethene, although the rather short carbon−carbon double bond should be a result of less effective back-donation due to the distorted structure as discussed above. A formal addition reaction of a diruthenium species to the C≡C bond in the ethynediyl complex **2*** should lead to the coordinatively saturated permetalated ethene structure **5*** with 66 cluster valence electrons (CVE) (Scheme 3).

Recently Kousantonis et al. reported the syntheses of the (η^5-C_5H_4R)Ru analogues of **5***, [(η^5-C_5H_4R)Ru]$_2$-$Ru_2(\mu_4$-$C_2)(CO)_{10}$ (**7**) [R = H (*cis*-**7a**), Me (*trans*-**7b**)], via addition of a mononuclear species, Ru(ethene)$(CO)_4$, to the μ-ethynediyldiruthenium complexes (η^5-C_5H_4R)$(CO)_2$-Ru−C≡C−Ru(η^5-C_5H_4R)$(CO)_2$ [14] (cis and trans refer to configuration of the two η^5-C_5H_4R rings with respect to the $Ru_4(\mu_4$-$C_2)$ moiety). The features for the $M_4(\mu_4$-$C_2)$ cores [C−C: 1.258(5) (*cis*-**7a**), 1.252(4), 1.258(4) Å (*trans*-**7b** with two independent molecules); δ_C 154.9 (*cis*-**7a**), 157.1 (*trans*-**7b**)] are essentially the same as those of **5***, and the twisting of the $M_4(\mu_4$-$C_2)$ core is correlated to the configuration of the cyclopentadienyl rings. The Ru_4C_2 core in *cis*-**7a** is more closely planar compared to those in *trans*-**7b**. The authors proposed that the permetalated ethene structure was formed via sequential addition of a mononuclear species, $Ru(CO)_n$, because the reaction afforded both cis and trans isomers, which were not interconverted with each other.

The second product **6*** (Figure 3) has been characterized as an octanuclear compound containing the two C_2 units. The metal array is based on the central Ru_4 square (Ru1−Ru2−Ru3−Ru4), each edge of which is bridged by either the Fe or Ru atom, and the bridging metal atoms are located alternately above and below the Ru_4 square. The C_2 ligand bridges the Fe and Ru centers projected to the same side to interact with the boat-shaped $FeRu_5$ metal framework. The two C_2 rods above and below the Ru_4 plane are arranged perpendicular to each other, as can be seen from a top view of the core part (Figure 3c).

When the bonding interaction of the C_2 bridge is inspected in detail, the C−C distances [C1−C2, 1.334-(8) Å; C3−C4, 1.354(7) Å] are further longer than the C−C distances in **5*** and **2**# but are found to be comparable to C(sp)−C(sp) single bond lengths [cf. butadiyne: 1.384(2) Å].[13,15] The distances from the C_2 carbon atoms to the out-of-plane metals (Fe1, Fe2, Ru5, Ru6) [C1−Fe1, 1.908(6) Å; C2−Ru5, 1.997(6) Å; C3−Fe2, 1.866(5) Å; C4−Ru6, 1.993(5) Å] are in the ranges of typical σ bond lengths, and the slightly longer C_2−Ru1−4 distances [2.123−2.205(6) Å] indicate contribution of π-bonding interactions between the C_2 ligand and the Ru_4 square. Although connection of two corners of the two metal triangles by two metal−metal bonds forms the distorted boat-shaped core structure, the C_2−metal bonds are basically σ bonds, and therefore, the C_2M_6 moieties can be described as a *permetalated ethane*. The bis(dicarbide) cluster compound **6*** is found to be coordinatively saturated judging from the number of its cluster valence electrons (124 e).

(12) Colborn, R. E.; Davies, D. L.; Dyke, A. F.; Endesfelder, A.; Knox, S. A. R.; Orpen, A. G.; Plaas, D. *J. Chem. Soc., Dalton Trans.* **1983**, 2661.

(13) March, J. *Advanced Organic Chemistry*, 3rd ed.; John Wiley and Sons: New York, 1985.

(14) (a) Byrne, L. T.; Hos, J. P.; Kousantonis, G. A.; Skelton, B. W. *J. Organomet. Chem.* **1999**, *592*, 95. (b) Byrne, L. T.; Hos, J. P.; Kousantonis, G. A.; Skelton, B. W.; White, A. H. *J. Organomet. Chem.* **2000**, *598*, 28.

(15) (a) Tanimoto, M.; Kuchitsu, K.; Morino, Y. *Bull. Chem. Soc. Jpn.* **1971**, *44*, 386. (b) Hölzl, F.; Wrackmayer, B. *J. Organomet. Chem.* **1979**, *179*, 394.

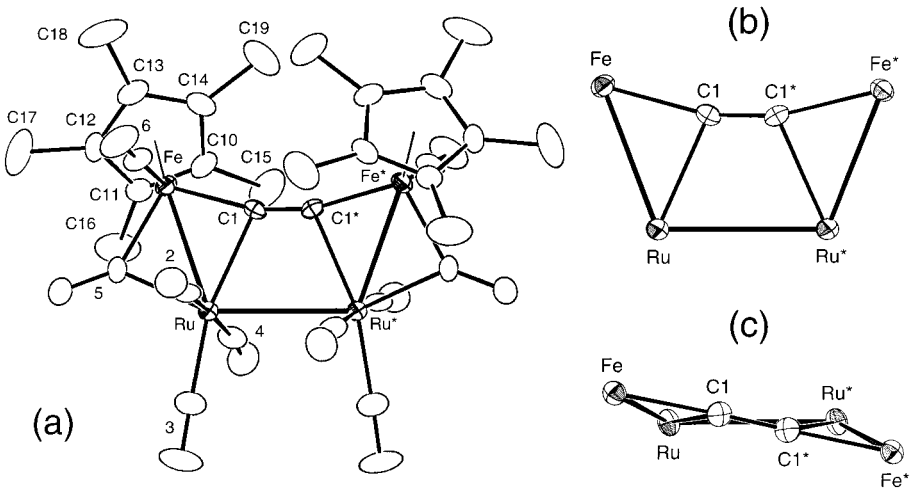

Figure 2. Molecular structure of **5*** drawn (with displacement ellipsoid amplitudes) at the 30% probability level, where labels without atom names are for CO ligands: (a) overview; (b) side view of the core part; (c) top view of the core part.

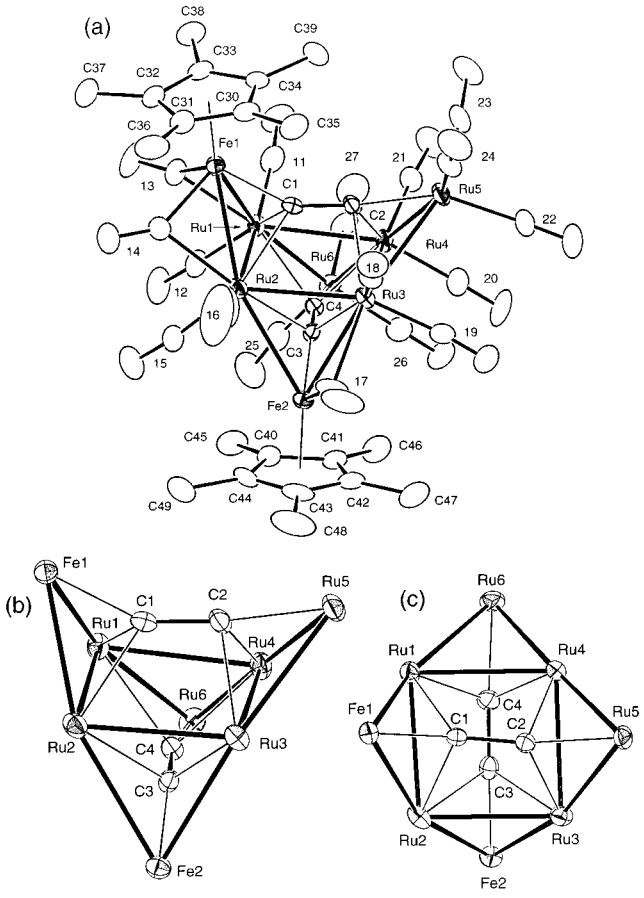

Figure 3. Molecular structure of **6*** drawn (with displacement ellipsoid amplitudes) at the 30% probability level, where labels without atom names are for CO ligands: (a) overview; (b) overview of the core part; (c) top view of the core part.

Table 2. Selected Structural Parameters for 5*

Bond Lengths (Å)			
C1−C1*	1.24(1)	Ru−C3	1.885(8)
C1−Fe	1.946(7)	Ru−C4	1.905(9)
C1−Ru	2.204(7)	Ru−C5	2.047(8)
Ru−Ru*	2.963(2)	Fe−C5	1.932(8)
Ru−Fe	2.733(2)	Fe−C6	1.740(8)
Ru−C2	1.933(9)		
Bond Angles (deg)			
Ru−C1−C1*	112.0(2)	C2−Ru−C3	88.5(3)
Fe−C1−C1*	165.5(2)	C2−Ru−C4	174.2(3)
Ru−C1−Fe	82.1(2)	C2−Ru−C5	90.0(3)
Ru*−Ru−Fe	110.61(4)	C3−Ru−C4	86.5(4)
Ru*−Ru−C1	66.5(2)	C3−Ru−C5	105.7(4)
Ru*−Ru−C2	92.7(2)	C4−Ru−C5	94.1(3)
Ru*−Ru−C3	98.7(3)	Ru−Fe−C1	53.0(2)
Ru*−Ru−C4	85.3(3)	Ru−Fe−C5	48.4(2)
Ru*−Ru−C5	155.5(2)	Ru−Fe−C6	95.5(3)
Fe−Ru−C1	44.9(2)	C1−Fe−C5	100.9(3)
Fe−Ru−C2	93.0(2)	C1−Fe−C6	90.9(4)
Fe−Ru−C3	150.5(3)	C5−Fe−C6	88.8(4)
Fe−Ru−C4	92.8(3)	Ru−C−O	173.9 −
Fe−Ru−C5	44.9(2)		178.5(9)
C1−Ru−C2	87.5(3)	Ru−C5−Fe	86.7(3)
C1−Ru−C3	164.4(3)	Ru−C5−O5	134.2(7)
C1−Ru−C4	96.7(3)	Fe−C5−O5	139.0(7)
C1−Ru−C5	89.4(3)	Fe−C6−O6	179.3(8)

A ^{13}C NMR spectrum of **6*** observed at 25 °C (Figure 4a,b) contains one set of Cp* signals and seven quaternary carbon signals, suggesting the occurrence of dynamic behavior. Below −60 °C, 10 quaternary carbon signals are observed in addition to the Cp* signals, for which no apparent change is noted (Figure 4c). First of all, the C_2 signals (δ_C 203.2, 209.0) are assigned by comparison with a sample obtained from ^{13}CO-enriched $Ru_3(CO)_{12}$ (Figure 4d).[16] The remaining eight signals are, therefore, due to M−CO (seven η^1-CO and one μ-CO). These spectral features can be interpreted in terms of the mechanism shown in Scheme 4. The inconsistency between the apparent C_2-symmetrical NMR feature and the X-ray structure with no element of symmetry can be explained by the fast switching of the two bridging carbonyl ligands (indicated as B and B′) attached to Ru_A (process a). The switching is not frozen even at −80 °C, and signals for B and B′ are not detected in the temperature range 25 to −80 °C because of broadening. The three signals observed at low temperatures (Figure 3c) can be assigned to the CO ligands (F−H) attached to Ru_C, which are not observed at 25 °C because of the $Ru_C(CO)_3$ rotation (process b) occurring at a rate faster than the NMR time scale. Thus, the seven quaternary signals observed at 25 °C are due to C1, C2, A, C, D, E, and I, and freezing of the

(16) The ^{13}C NMR signals for the C_2 ligands of **6*** were reported.[8c] But careful reexamination of ^{13}C NMR measurements revealed that they were due to impurities and the signals could not be located at ambient temperature because of the dynamic processes.

Table 3. Selected Structural Parameters for 6*

Bond Lengths (Å)					
C1−C2	1.334(8)	C4−Ru6	1.993(5)	C13−Ru1	2.189(7)
C3−C4	1.354(7)	Ru1−Ru2	2.7710(6)	C13−Fe1	1.879(8)
C1−Fe1	1.908(6)	Ru1−Ru4	2.8466(7)	C14−Fe1	1.874(7)
C1−Ru1	2.205(6)	Ru1−Ru6	2.8286(6)	C14−Ru2	2.184(8)
C1−Ru2	2.181(6)	Ru1−Fe1	2.711(1)	C17−Ru3	2.373(8)
C2−Ru3	2.147(6)	Ru2−Ru3	2.8383(7)	C17−Fe2	1.780(8)
C2−Ru4	2.142(6)	Ru2−Fe1	2.7252(9)	Ru−CO	1.866−1.968(8)
C2−Ru5	1.997(6)	Ru2−Fe2	2.8442(9)	Fe−C(Cp*)	2.086−2.139(7)
C3−Fe2	1.866(5)	Ru3−Ru4	2.8501(6)	C13−O13	1.16(1)
C3−Ru2	2.202(5)	Ru3−Ru5	2.815(1)	C14−O14	1.17(1)
C3−Ru3	2.187(6)	Ru3−Fe2	2.677(1)	C17−O17	1.17(1)
C4−Ru1	2.183(6)	Ru4−Ru5	2.7513(9)	C−O	1.11−1.16(1)
C4−Ru4	2.123(6)	Ru4−Ru6	2.7518(7)		
Bond Angles (deg)					
Ru1−C1−Ru2	78.3(2)	Ru1−C4−C3	108.3(4)	Ru5−Ru3−Fe2	160.76(3)
Ru1−C1−Fe1	82.1(2)	Ru4−C4−Ru6	83.9(2)	Ru1−Ru4−Ru3	91.64(2)
Ru1−C1−C2	120.6(4)	Ru4−C4−C3	98.6(4)	Ru1−Ru4−Ru5	120.63(2)
Ru2−C1−Fe1	83.3(2)	Ru6−C4−C3	166.6(4)	Ru1−Ru4−Ru6	60.67(2)
Ru2−C1−C2	120.4(4)	Ru2−Ru1−Ru4	87.99(2)	Ru3−Ru4−Ru5	60.31(2)
Fe1−C1−C2	148.5(5)	Ru2−Ru1−Ru6	115.53(2)	Ru3−Ru4−Ru6	121.62(2)
Ru3−C2−Ru4	83.3(2)	Ru2−Ru1−Fe1	59.60(2)	Ru5−Ru4−Ru6	177.93(2)
Ru3−C2−Ru5	85.5(2)	Ru4−Ru1−Ru6	58.01(2)	Ru3−Ru5−Ru4	61.58(2)
Ru3−C2−C1	100.5(4)	Ru4−Ru1−Fe1	106.11(3)	Ru1−Ru6−Ru4	61.32(2)
Ru4−C2−Ru5	83.3(2)	Ru6−Ru1−Fe1	164.12(3)	Ru1−Fe1−Ru2	61.29(2)
Ru4−C2−C1	99.8(4)	Ru1−Ru2−Ru3	93.48(2)	Ru2−Fe2−Ru3	61.79(2)
Ru5−C2−C1	173.5(5)	Ru1−Ru2−Fe1	59.11(2)	Ru1−C13−O13	132.3(6)
Ru2−C3−Ru3	80.6(2)	Ru1−Ru2−Fe2	110.14(2)	Fe1−C13−O13	144.4(6)
Ru2−C3−Fe2	88.3(2)	Ru3−Ru2−Fe1	105.67(3)	Ru2−C14−O14	132.4(6)
Ru2−C3−C4	108.8(4)	Ru3−Ru2−Fe2	56.20(2)	Fe1−C14−O14	143.5(7)
Ru3−C3−Fe2	82.2(2)	Fe1−Ru2−Fe2	160.08(3)	Ru3−C17−O17	124.9(7)
Ru3−C3−C4	122.1(4)	Ru2−Ru3−Ru4	86.63(2)	Fe2−C17−O17	156.1(8)
Fe2−C3−C4	151.5(5)	Ru2−Ru3−Ru5	119.78(2)	Ru−C−O	173.2−178.6(7)
Ru1−C4−Ru4	82.8(2)	Ru4−Ru3−Ru5	58.10(2)		
Ru1−C4−Ru6	85.1(2)	Ru4−Ru3−Fe2	104.30(3)		

Scheme 3

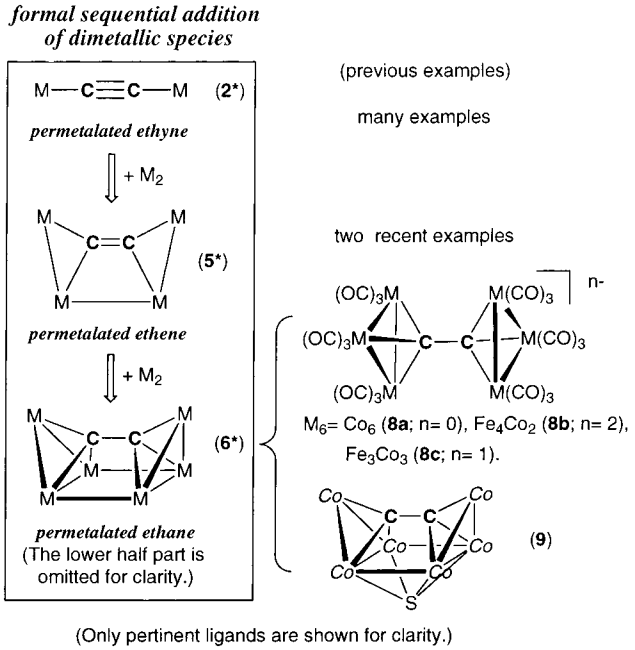

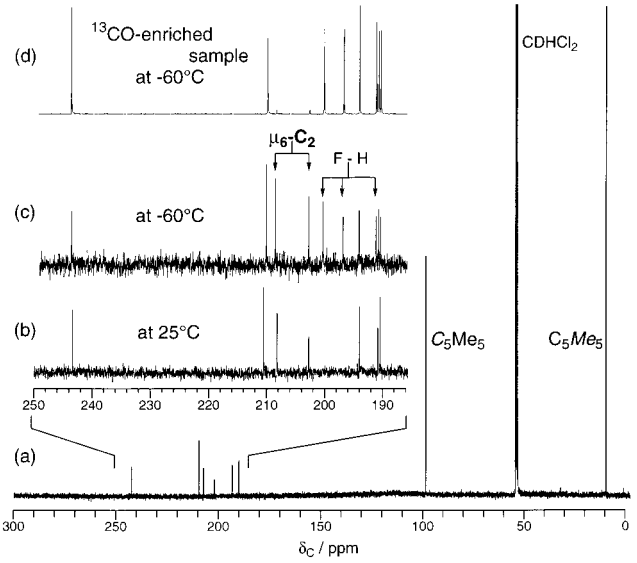

Figure 4. ^{13}C NMR spectra of **6*** observed at 100 MHz: (a) full spectrum observed at 25 °C; (b) expanded spectrum of (a); (c) expanded spectrum, observed at −60 °C; (d) expended spectrum of a ^{13}CO-enriched sample, observed at −60 °C.

$Ru_C(CO)_3$ rotation at low temperatures causes the appearance of 10 signals (C1, C2, A, C, D, E, F, G, H, and I). The C_2 signals are shielded compared to those of **8b** (δ_C 279.4, 285.7) and **8c** (δ_C 285.9, 293.7), the chemical shifts of which are typical for μ_3-alkylidyne carbon atoms.[17]

The first example of a permetalated ethane, $Co_6(\mu_6\text{-}C_2)(CO)_{18}$ (**8a**), was isolated from a mixture resulting from thermolysis of the μ_3-bromomethylidyne tricobalt cluster compound $(\mu_3\text{-}BrC)Co_3(CO)_9$, as reported by Ercoli in 1966[5a] and later structurally characterized by Penfold.[5b] The metal framework consists of two separated Co_3 triangles, which are bridged by the C_2 ligand. Later isoelectronic anionic Fe,Co mixed-metal cluster compounds $[Fe_4Co_2(\mu_6\text{-}C_2)(CO)_{18}]^{2-}$ (**8b**) and $[Fe_3Co_3(\mu_6\text{-}$

(17) Mann, B. E.; Taylor, B. F. *^{13}C NMR Data for Organometallic Compounds*; Academic Press: London, 1981.

Scheme 4

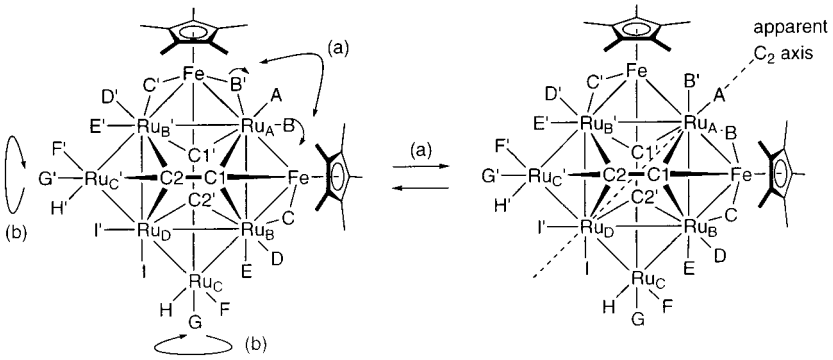

$C_2)(CO)_{18}]^-$ (**8c**) were synthesized via a different route (metal addition to an Fe_4−acetylide cluster type C_2 complex) by Shriver.[5c] A Co_6 cluster compound with the metal framework very similar to the upper half of **6**, $Co_6(\mu_6\text{-}C_2)(\mu_4\text{-}S)(CO)_{14}$ (**9**), was isolated from a reaction mixture of $Co_2(CO)_8$ and CS_2 as reported by Stangellini.[5e] Their C−C lengths [1.37(1) Å (**8a**), 1.362(8) Å (**8b**), 1.37(2) Å (**9**)] are comparable to that of **6***.

When the reaction of **2*** with $Ru_3(CO)_{12}$ was monitored by ^{1}H NMR, the permetalated ethene **5*** appeared first and subsequently the acetylide **3*** and the permetalated ethane **6*** were gradually formed. In addition, complex **5*** was found to be thermally less stable than **3*** and **6***. These observations suggest that the permetalated ethane **6*** may be formed by addition of a ruthenium species to **5*** or thermal dimerization of the $FeRu_3(\mu\text{-}C_2)$ core in **3***. To confirm these possibilities, reaction of an isolated sample of **5*** with $Ru_3(CO)_1$ (eq 2) and thermolysis of **3*** (eq 3) were examined. As a

$$\mathbf{5^*} + Ru_3(CO)_{12} \xrightarrow[\text{refluxing toluene}]{} \mathbf{3^*}\ (50\%) + \mathbf{6^*}\ (20\%) \quad (2)$$

$$\mathbf{3^*} \xrightarrow[\text{refluxing toluene}]{} \mathbf{6^*}\ (42\%) \quad (3)$$

result, reaction of **5*** with $Ru_3(CO)_{12}$ in refluxing toluene (eq 2) afforded permetalated ethane **6*** in addition to the acetylide cluster compound **3*** (Scheme 3). Furthermore, **5*** and **6*** were isolated in better yields by carrying out the reactions in refluxing benzene and toluene, respectively (eqs 4 and 5; see Experimental Section). It should be noted that thermolysis of **5*** in

$$\mathbf{2^*} + Ru_3(CO)_{12} \xrightarrow[\text{refluxing toluene}]{} \mathbf{5^*}\ (59\%\ \text{isolated yield}) \quad (4)$$

$$\mathbf{2^*} + Ru_3(CO)_{12} \xrightarrow[\text{refluxing toluene}]{} \mathbf{6^*}\ (26\%\ \text{isolated yield}) \quad (5)$$

the absence of $Ru_3(CO)_{12}$ afforded an intractable mixture of products in which neither **5*** nor **6*** was detected. Furthermore, thermolysis of **3*** in refluxing toluene (eq 3) resulted in dimerization of its $FeRu_3(\mu\text{-}C_2)$ core to give the permetalated ethane **6*** with the doubled core composition $Fe_2Ru_6(\mu\text{-}C_4)_2$ in 42% yield (eq 3). Thus, the octanuclear permetalated ethane structure **6*** turns out to be a thermodynamic sink in the present reaction system and can be formed via condensation of lower nuclearity C_2 cluster compounds.

Scheme 5

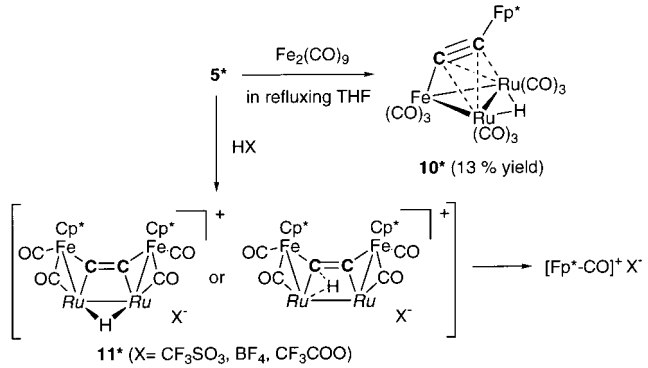

We attempted addition of another group 8 metal carbonyl species, $Fe_2(CO)_9$, to **5***.[18] The reaction was sluggish, and after the mixture was refluxed in THF for 15 h a small amount of acetylide cluster compound **10*** was obtained (Scheme 5). Complex **10*** showed spectral features (see Experimental Section) essentially the same as those of **3*** and was characterized as an Fe-substituted derivative of **3*** as revealed by X-ray crystallography.[19] In **10***, the Ru atom σ-bonded to the C_2 ligand in **3*** (Ru1) is replaced by the Fe atom (Fe1). This result suggests that the Ru acetylide cluster compound **3*** is also formed via an analogous addition reaction of an $Ru(CO)_n$ species with **5***.

We also examined the reaction of **5*** with a proton, a small electrophile, which may directly add to the sterically congested C_2 moiety (Scheme 5). Addition of CF_3SO_3H, $HBF_4{\cdot}OEt_2$, or CF_3COOH to a CH_2Cl_2 solution of **5*** caused an immediate color change from purple to red-purple and a shift of CO vibrations toward the higher energy region, suggesting formation of a cationic species. ^{1}H NMR spectra of mixtures obtained from CF_3SO_3H and $HBF_4{\cdot}OEt_2$ showed one hydride and two Cp* signals [$\delta_H(CD_2Cl_2)$ −8.03 (H), 1.91, 1.90 (Cp*)], whereas protonation with CF_3COOH gave a spectrum with a similar pattern but with different chemical shift values [$\delta_H(CD_2Cl_2)$ −4.13 (H), 1.94, 1.81 (Cp*)]. These spectral features are consistent with either of the structures **11*** shown in Scheme 5, the side-bound bridging hydride complex or the species with an agostic $C_2\cdots H\cdots Ru$ interaction. Complex **11*** was unstable, and attempted isolation resulted in fragmentation of the

(18) Attempted reactions of **5** with $Co_2(CO)_9$, $Pt(CH_2{=}CH_2)(PPh_3)_2$, $[Rh(CH_2{=}CH_2)_2(\mu\text{-}Cl)]_2$, $Cp^*Rh(CO)_2$, $(\eta^5\text{-}C_5H_4Me)(CO)_2$, and $Mn_2(CO)_{10}$ afforded a complicated mixture of products from which no characterizable product could be isolated.

(19) An ORTEP view of **10*** is included in Supporting Information.

cluster structure to give [Fp*−CO]X as the only isolable product.

Structure Expansion of Acetylide Cluster Type Tetranuclear Dicarbide Cluster Compounds with Cp Ligand (3) via Thermolysis and Oxidation. Cp derivatives of the higher nuclearity dicarbide cluster compounds would be obtained from the Cp derivative of the ethynediyl complex **2**, but synthesis of **2** has been unsuccessful until now. Then the thermal condensation of the $FeRu_3(\mu\text{-}C_2)$ core observed for the Cp* cluster compound **3*** (eqs 2 and 3) prompted us to examine similar coupling reactions of the Cp derivative **3**.

(i) Thermolysis. Thermolysis of **3** in refluxing toluene followed by silica gel TLC separation afforded two products **6** and **12** resulting from dimerization of the $FeRu_3(\mu\text{-}C_2)$ core in low yields (eq 6). One was characterized as the dicarbide cluster compound **6** on the basis of FAB-MS and IR data, which are shown in Figure 5. The isotopomer distribution of the molecular ion peaks for **6** is in very good agreement with the calculated one, and fragment peaks due to loss of up to 17 carbonyl ligands are observed (Figure 5a). These data support the composition of **6** to be "$Cp_2Fe_2Ru_2(\mu\text{-}C_2)_2(CO)_{17}$" [cf. **6***: $Cp^*_2Fe_2Ru_2(\mu\text{-}C_2)_2(CO)_{17}$]. Furthermore, the pattern of CO vibrations of **6** (Figure 5b) is very similar to that of **6*** and they were shifted toward higher energy region because of less electron-donating ability of the Cp ligands compared to the Cp* ligands in **6***. Although X-ray crystallographic analysis revealed the presence of an $Fe_2Ru_6(\mu_6\text{-}C_2)_2$ core similar to that in **6***, the structure could not be refined because of severe disorder of a part of the metal components. Combined with the ^{1}H NMR data containing only one singlet Cp signal (δ_H 4.71), it is concluded that **6** is the Cp derivative of the bis(dicarbide) cluster compound **6***.

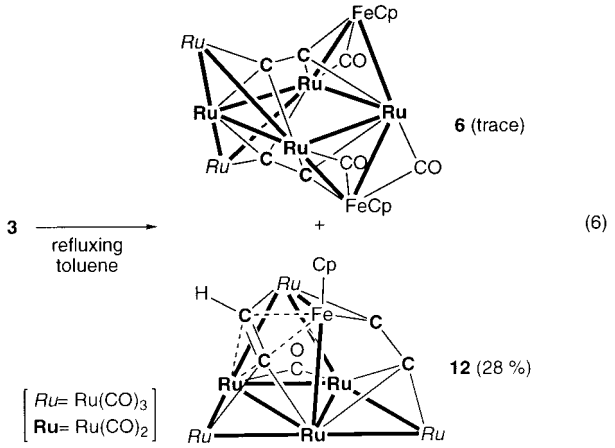

The other product **12** showing the deshielded ^{1}H NMR signal (δ 8.64) was a heptanuclear $FeRu_6$ complex containing one C_2 and one C_2H ligand as revealed by X-ray crystallography (Figure 6 and Table 4). The metal core (Figure 6b) consists of the flat W-shaped raftlike Ru_5 framework [Ru(1−5)], which is fused with the FeRu(1,3,6) square. In addition, the Ru(3,4,6) moiety forms a triangular structure, although the Ru4−Ru6 separation [3.056(1) Å] is substantially longer than the other Ru−Ru lengths [2.7575(8)−2.9759(9) Å]. Complex **12** is a coordinatively saturated 104 CVE species when C_2H and C_2 ligands are regarded as five- and six-electron donors, respectively. The C_2 ligand [C1−C2: 1.334(9) Å] interacts with the FeRu(1,2,3,6) envelope in the coordination mode, similar to that observed for $(\mu_5\text{-}C_2)Ru_5(\mu\text{-}SMe)_2(\mu\text{-}PPh_2)_2$ [C−C: 1.305(5) Å].[5h] The C_2H moiety [C3−C4: 1.420(9) Å] can be viewed as a trimetalated [Ru(1,5,6)] ethene, which is sandwiched between Fe and Ru(4) through π interactions. We attempted the determination of the origin of the $\mu_5\text{-}C_2H$ atom by conducting the thermolysis in toluene-d_8, but it was unsuccessful because of H−D exchange of the bridging hydride in **3** prior to its conversion.

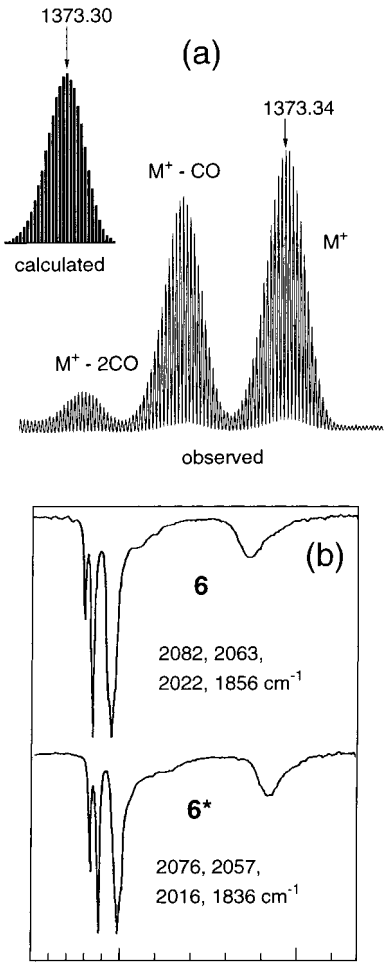

Figure 5. FAB-MS and IR spectra for **6**: (a) FAB-MS spectrum ([$M^+ - nCO$] region, $n = 0-2$) and a spectrum calculated for M^+; (b) comparison of IR spectra of **6** and **6*** (ν_{CO} region).

(ii) Oxidation of Anionic Dicarbide Cluster. Redox condensation is another typical synthetic method of higher nuclearity cluster compounds together with the thermolysis discussed above.[20] An extended structure may be formed via coupling of a radical species generated by one-electron oxidation of the anionic cluster compound **13**, which was prepared from **3** following the procedure reported for an organic counterpart, PPh_4-$[Ru_3(CO)_9(\mu\text{-}H)(\mu_3\text{-}C{\equiv}C{-}Bu^t)]$ **14**, obtained from **4**.[21]

(20) (a) *Comprehensive Organometallic Chemistry II*; Abel, E. W., Stone, F. G. A., Wilkinson, G., Eds.; Pergamon: Oxford, 1995; Vol. 10, Chapter 3. (b) Shriver, D. F.; Kaesz, H.; Adams, R. D. *The Chemistry of Metal Cluster Complexes*; VCH: New York, 1990. (c) *Metal Clusters in Chemistry*; Braunstein, P., Oro, L. A., Raithby, P. R., Eds.; Wiley-VCH: Weinheim, Germany, 1999; Vols. 1−3. (d) Structure expansion of dicarbide clusters by addition of metal fragments has also been studied by Bruce et al. Adams, C. J.; Bruce, M. I.; Skelton, B. W.; White, A. H. *J. Chem. Soc., Chem. Commun.* **1993**, 446 and references therein.

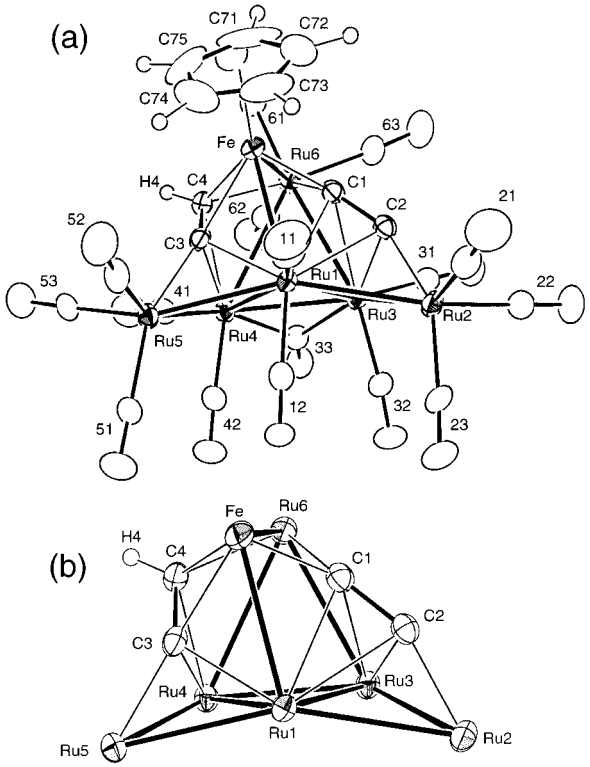

Figure 6. Molecular structure of **12** drawn (with displacement ellipsoid amplitudes) at the 30% probability level, where labels without atom names are for CO ligands: (a) overview; (b) overview of the core part.

Scheme 6

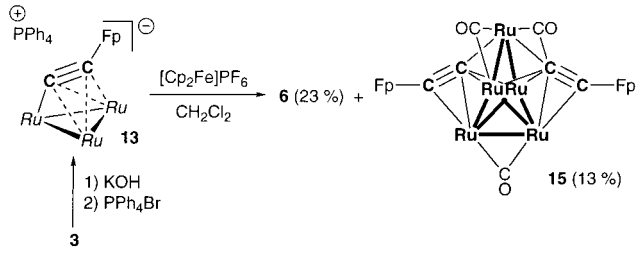

Treatment of **13** with 1 equiv of $[Cp_2Fe]PF_6$ gave a mixture of products from which two higher nuclearity cluster compounds **6** and **15** were isolated and characterized (Scheme 6).

One of the products was characterized as the bis(dicarbide) cluster compound **6** by comparison of its spectral features with those of an authentic sample. The other product **15** characterized by X-ray crystallography turned out to be a heptanuclear bis(dicarbide) cluster compound with the arrowhead-shaped Ru_5 core of C_2 symmetry (Figure 7). A unit cell of **15** contains two crystallographically independent molecules with essentially the same geometry, one of which sits on a crystallographically imposed site. The FpC_2 groups interact with the Ru_4 butterfly parts as acetylide ligands, and the Fe atoms are not incorporated in the central cluster structure. Complex **15** with no Ru(2)···Ru(4) bonding interaction [3.477(2) Å (molecule 1); 3.472(2) Å (molecule 2)] belongs to a rare class of arrowhead M_5 cluster compounds without an encapsulated atom (usually μ_5-C),[20b] and in contrast to the previously reported acetylide clusters where the C≡C part interacts with the top metal atom, the dicarbide parts in **5*** are π-coordinated to the bottom-edge Ru atoms.[22] The heptanuclear complex **15** is a coordinatively saturated 112 CVE species with two six-electron-donating C_2 ligands. Thus, the $(C_2)FeRu_3$ cores in **3** and **13** are coupled upon thermolysis and oxidation, respectively, to afford the higher nuclearity cluster compounds **6**, **12**, and **15**.

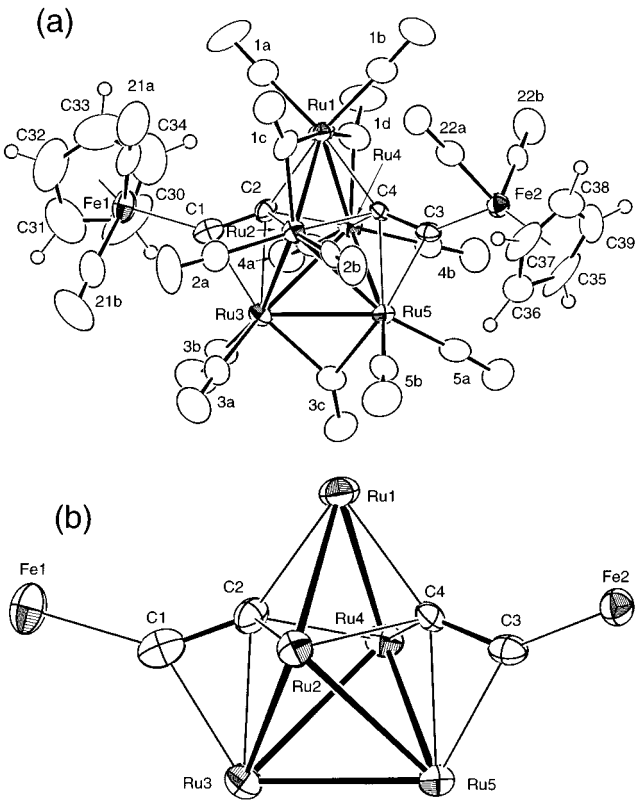

Figure 7. Molecular structure of **15** (molecule 1) drawn (with displacement ellipsoid amplitudes) at the 30% probability level, where labels without atom names are for CO ligands: (a) overview; (b) overview of the core part.

Comparison of Structures of the $M_3(CO)_9(\mu$-X)-(μ-C≡C−FP) Type Tetranuclear Acetylide Cluster Compounds [M = Fe, Ru; X = H, Anion]. Through the present study several $M_3(CO)_9(\mu$-X)(μ-C≡C−FP) type tetranuclear acetylide cluster compounds **3**, **4**, **10***, and **13** are obtained, and their structural parameters are compared together with related organic counterparts (**4** and **14**) and the tetrairon analogue (**16**) as shown in Table 1. Complex **16** was obtained by nucleophilic replacement of $(PPN)_2[Fe_3(CO)_9(\mu_3$-C≡C−OAc)] by NaFp as reported by Shriver.[5d] The coordination modes of the M4−C_2 parts and the structure of the $M_3(CO)_9$ core parts in these complexes are very similar; the C≡C−M4 moiety interacts with M1 and M2,3 through η^1 and η^2 modes, respectively. As for the ruthenium derivatives where M2 and M3 equal Ru, the C≡C and M2−M3 distances could be divided into two groups, those in neutral and those in anionic cluster compounds. The C≡C distances in the anionic complexes are shorter

(21) Barner-Thorsen, C.; Hardcastle, K. I.; Rosenberg, E.; Siegel, J.; Landfredi, A. M. M.; Tiripicchio, A.; Camellini, M. T. *Inorg. Chem.* **1981**, *20*, 4306.

(22) (a) Farrar, D. H.; John, G. R.; Johnson, B. F. G.; Lewis, J.; Raithby, P. R.; Rosales, M. *J. J. Chem. Soc., Chem. Commun.* **1981**, 886. (b) Lanfranchi, M.; Tiripicchio, A.; Sappa, E.; MacLaughlin, A.; Carty, A. J. *J. Chem. Soc., Chem. Commun.* **1982**, 538.

Table 4. Selected Structural Parameters for 12

		Bond Lengths (Å)			
C1−C2	1.334(9)	C3−Fe	2.012(7)	Ru1−Ru4	2.8927(8)
C1−Ru1	2.282(7)	C3−Ru4	2.253(6)	Ru1−Ru5	2.8075(9)
C1−Ru6	2.191(6)	C3−Ru5	1.964(7)	Ru1−Fe	2.754(1)
C1−Fe	1.877(7)	C4−Ru4	2.317(7)	Ru2−Ru3	2.7864(8)
C2−Ru1	2.263(7)	C4−Ru6	2.133(7)	Ru3−Ru4	2.7575(8)
C2−Ru2	1.939(6)	C4−Fe	2.031(7)	Ru3−Ru6	2.9759(9)
C2−Ru3	2.180(6)	Ru1−Ru2	2.844(1)	Ru4−Ru5	2.814(1)
C3−C4	1.420(9)	Ru1−Ru2	2.8436(8)	Ru4−Ru6	3.056(1)
C3−Ru1	2.141(6)	Ru1−Ru3	2.7764(9)	Ru6−Fe	2.675(1)
		Bond Angles (deg)			
C2−C1− Ru1	72.2(4)	C3−C4−Fe	68.7(4)	Ru4−Ru3−Ru6	64.30(3)
C2−C1−Ru6	134.9(5)	Ru4−C4−Ru6	86.7(3)	C3−Ru4−C4	36.2(2)
C2−C1−Fe	141.7(5)	Ru4−C4−Fe	118.6(3)	C3−Ru4−Ru1	47.2(2)
Ru1−C1−Ru6	116.1(3)	Ru6−C4−Fe	79.9(3)	C3−Ru4−Ru3	95.7(2)
Ru1−C1−Fe	82.3(3)	C2−Ru1−C3	111.6(2)	C3−Ru4−Ru5	43.9(2)
Ru6−C1−Fe	81.9(2)	C2−Ru1−Ru4	100.9(1)	C3−Ru4−Ru6	70.4(2)
C1−C2−Ru1	73.7(4)	C2−Ru1−Ru5	154.6(2)	C4−Ru4−Ru1	74.3(2)
C1−C2−Ru2	158.1(6)	C2−Ru1−Fe	73.8(2)	C4−Ru4−Ru3	96.6(2)
C1−C2−Ru3	86.2(4)	C3−Ru1−Ru5	44.3(2)	C4−Ru4−Ru5	75.3(2)
Ru1−C2−Ru2	84.8(2)	C3−Ru1−Fe	46.5(2)	C4−Ru4−Ru6	44.2(2)
Ru1−C2−Ru3	77.3(2)	C3−Ru1−Ru4	50.5(2)	Ru1−Ru4−Ru3	58.81(2)
Ru2−C2−Ru3	84.9(3)	C2−Ru2−Ru1	52.4(2)	Ru1−Ru4−Ru5	58.93(2)
C4−C3− Ru1	125.2(5)	C2−Ru2−Ru3	51.2(2)	Ru1−Ru4−Ru6	79.22(3)
C4−C3−Ru4	74.4(4)	C2−Ru3−Ru1	52.7(2)	Ru3−Ru4−Ru5	117.01(2)
C4−C3−Ru5	137.2(5)	C2−Ru3−Ru2	43.9(2)	Ru3−Ru4−Ru6	61.32(2)
C4−C3−Fe	70.2(4)	C2−Ru3−Ru4	107.5(2)	Ru5−Ru4−Ru6	114.31(3)
Ru1−C3−Ru4	82.3(2)	C2−Ru3−Ru6	77.1(2)	Ru1−Ru5−Ru4	61.94(2)
Ru1−C3−Ru5	86.2(2)	Ru5−Ru1−Fe	87.33(3)	C3−Ru5−Ru1	49.6(2)
Ru1−C3−Fe	83.0(2)	Ru1−Ru2−Ru3	59.09(2)	C3−Ru5−Ru4	52.7(2)
Ru4−C3−Ru5	83.4(2)	Ru1−Ru3−Ru2	61.48(2)	Ru3−Ru6−Ru4	54.38(2)
Ru4−C3−Fe	122.6(3)	Ru1−Ru3−Ru4	63.03(2)	Ru3−Ru6−Fe	91.09(3)
Ru5−C3−Fe	149.9(3)	Ru1−Ru3−Ru6	82.48(3)	C1−Ru6−Ru3	54.8(2)
C3−C4− Ru4	69.5(4)	Ru2−Ru3−Ru4	122.37(3)	C4−Ru6−Ru3	94.7(2)
C3−C4−Ru6	122.3(5)	Ru2−Ru3−Ru6	120.84(3)	Ru4−Ru6−Fe	81.23(4)
C1−Ru6−C4	80.5(3)	Ru1−Fe−Ru6	88.67(4)	C3 −Fe−C4	41.1(3)
C1−Ru6−Ru4	80.6(2)	C1−Fe−Ru1	55.2(2)	C3−Fe−Ru1	50.5(2)
C1−Ru6−Fe	44.0(2)	C1−Fe−C3	91.1(3)	C3−Fe−Ru6	82.5(2)
C4−Ru6−Ru4	49.2(2)	C1−Fe−C4	91.2(3)	C4−Fe−Ru1	81.7(2)
C4−Ru6−Fe	48.4(2)	C1−Fe−Ru6	54.2(2)	C4−Fe−Ru6	51.7(2)

Scheme 7

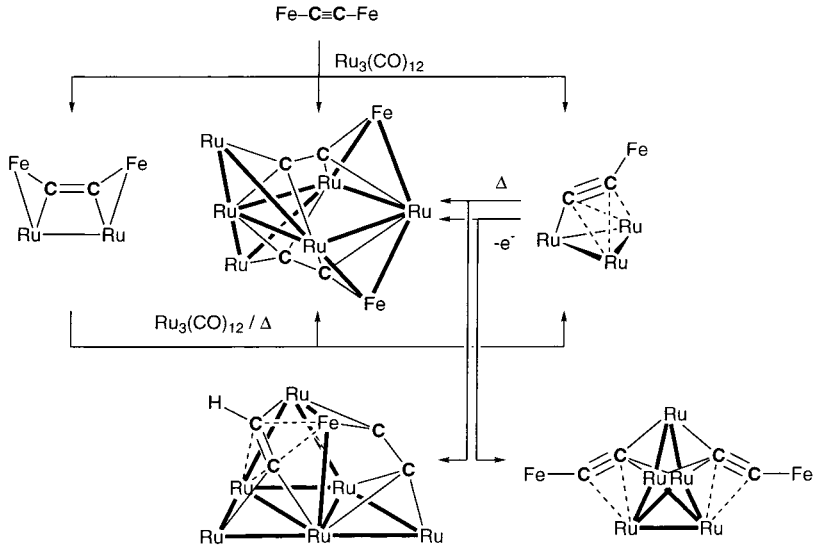

than those in the neutral complexes by ca. 0.05 Å, and in contrast, the M2−M3 distances in the anionic complexes are longer than those in the neutral complexes by ca. 0.1 Å. The former feature should be a result of weakened π donations from the acetylide ligand to the anionic trimetallic framework, and the latter is due to lack of the bridging hydride ligand in the anionic complexes. It is notable that no significant influence of the metal substituents (M4) on the C≡C moiety is detected when compared with the organic counterparts **4** and **14**. Thus, the M4 groups in **3**, **4**, **10***, **13**, and **16** work simply as acetylide substituents and no apparent communication is present between the M4 group and the triangular cluster part.

Conclusion

The cluster transformations described in the present paper are summarized in Scheme 7. As for the Cp*

Table 5. Selected Structural Parameters for 15[a]

molecule 1				molecule 2	
		Bond Lengths (Å)			
C1−C2	1.32(2)	C3−C4	1.34(2)	C5−C6	1.35(2)
C1−Fe1	1.93(2)	C3−Fe2	1.93(1)	C5−Fe11	1.89(1)
C1−Ru3	2.14(1)	C3−Ru5	2.14(1)	C5−Ru13	2.15(1)
C2−Ru1	2.14(1)	C4−Ru1	2.15(1)	C6−Ru11	2.18(1)
C2−Ru2	2.26(1)	C4−Ru2	2.24(1)	C6−Ru12	2.26(1)
C2−Ru3	2.26(1)	C4−Ru5	2.23(1)	C6−Ru13	2.23(1)
C2−Ru4	2.16(1)	C4−Ru4	2.16(1)	C6−Ru12*	2.15(1)
Ru1−Ru2	2.731(2)	Ru1−Ru4	2.708(2)	Ru11−Ru12	2.709(2)
Ru2−Ru3	2.905(2)	Ru4−Ru5	2.885(2)	Ru12−Ru13	2.875(2)
Ru2−Ru5	2.900(2)	Ru3−Ru4	2.916(2)	Ru12−Ru13*	2.944(2)
Ru3−Ru5	2.792(2)			Ru13−Ru13*	2.784(2)
terminal Ru−CO	1.87−1.91(2)			terminal Ru−CO	1.85−1.90(2)
bridging Ru−CO	1.92−2.18(2)			bridging Ru−CO	2.05−2.17(2)
terminal Fe−CO	1.70−1.78(2)			terminal Fe−CO	1.79(2)
		Bond Angles (deg)			
C2−C1−Fe1	144(1)	C4−C3−Fe2	143(1)	C6−C5−Fe11	145(1)
C2−C1−Ru3	78(1)	C4−C3−Ru5	76.1(8)	C6−C5−Ru13	75.3(8)
Fe1−C1−Ru3	138.5(8)	Fe2−C3−Ru5	141.2(7)	Fe11−C5−Ru13	139.9(8)
C1−C2−Ru1	146(1)	C3−C4−Ru1	145(1)	C5−C6−Ru11	144(1)
C1−C2−Ru4	130(1)	C3−C4−Ru4	131(1)	C5−C6−Ru12*	133(1)
C1−C2−Ru2	109.2(9)	C3−C4−Ru2	107.7(9)	C5−C6−Ru12	108(1)
C1−C2−Ru3	67.7(9)	C3−C4−Ru5	68.2(8)	C5−C6−Ru13	68.7(8)
Ru1−C2−Ru4	78.0(4)	Ru1−C4−Ru4	77.9(4)	Ru12−C6−Ru11	77.5(5)
Ru1−C2−Ru2	76.7(5)	Ru1−C4−Ru2	76.9(4)	Ru11−C6−Ru12*	75.2(4)
Ru1−C2−Ru3	144.8(7)	Ru1−C4−Ru5	145.1(7)	Ru11−C6−Ru13	144.2(6)
Ru4−C2−Ru2	103.7(6)	Ru4−C4−Ru2	104.3(5)	Ru12−C6−Ru12*	103.6(5)
Ru4−C2−Ru3	82.4(5)	Ru4−C4−Ru5	82.0(5)	Ru12−C6−Ru13	84.4(5)
Ru2−C2−Ru3	80.0(4)	Ru5−C4−Ru2	80.7(4)	Ru13−C6−Ru12*	79.6(4)
C2−Ru1−C4	74.8(5)			C6−Ru11−C6*	74.7(7)
C4−Ru2−C2	70.6(5)	C4−Ru4−C2	74.0(5)	C6−Ru12−C6*	73.4(5)
C1−Ru3−C2	34.7(5)	C3−Ru5−C4	35.7(5)	C5−Ru13−C6	36.0(5)
Ru4−Ru1−Ru2	79.49(5)			Ru12−Ru11−Ru12*	79.69(7)
Ru1−Ru2−Ru3	96.18(5)	Ru1−Ru2−Ru5	95.75(4)	Ru11−Ru12−Ru13*	95.65(5)
Ru1−Ru4−Ru3	96.44(5)	Ru1−Ru4−Ru5	96.62(5)	Ru11−Ru12−Ru13	97.28(5)
Ru5−Ru2−Ru3	57.50(4)	Ru5−Ru4−Ru3	57.54(4)	Ru13−Ru12−Ru13*	57.15(5)
Ru5−Ru3−Ru2	61.16(5)	Ru3−Ru5−Ru2	61.35(5)	Ru13*−Ru13−Ru12	62.68(4)
Ru5−Ru3−Ru4	60.67(4)	Ru3−Ru5−Ru4	61.79(4)	Ru13*−Ru13−Ru12*	60.17(4)
Ru4−Ru5−Ru2	73.90(4)	Ru2−Ru3−Ru4	73.36(4)	Ru12−Ru13−Ru12*	73.25(5)
terminal M−C−O	176−178(2)			terminal M−C−O	177−179(2)
Ru2−C1c−O1c	145(1)	Ru4−C1d−O1d	146(1)	Ru12−C11b−O11b	144(1)
Ru1−C1c−O1c	131(1)	Ru1−C1d−O1d	133(1)	Ru11−C11b−O11b	137(1)
Ru1−C1c−Ru2	83.3(7)	Ru1−C1d−Ru4	81.0(5)	Ru11−C11b−Ru12	79.9(6)
Ru3−C3c−O3c	140(1)			Ru13−C13c−O13c	138.9(5)
Ru5−C3c−O3c	136(1)			Ru13−C13c−O13c	138.9(5)
Ru5−C3c−Ru3	83.9(6)			Ru13−C13c−Ru13	82.3(9)

[a] With two independent molecules. Molecule 2 sits on a crystallographic C_2-symmetrical site.

system, the present study reveals that permetalated ethene and ethane structures result from formal sequential addition of dimetallic fragments to the C≡C triple bond in the ethynediyl complex, a permetalated ethyne (Scheme 3). Although the starting compounds **1**, **1***, and **2*** are acetylide complexes, the structural features of the obtained permetalated hydrocarbons characterized by X-ray crystallography are totally different from those of previously reported acetylide cluster compounds.[1] The higher nuclearity cluster compounds are also formed by thermal and redox condensation of the $FeRu_3(\mu\text{-}C_2)$ core in the acetylide cluster compound as revealed by the results of the Cp system. The results obtained would provide insights into the coordination modes of dicarbide species (C_2) on a heterogeneous catalyst surface.[2] The synthetic study on dicarbide (C_2) cluster compounds is now extended to polycarbon (C_{2n}) cluster compounds derived from related polyynediyl complexes, $M-(C{\equiv}C)_n-M$.[8k−p]

Experimental Section

General Methods. All manipulations were carried out under an inert atmosphere by using standard Schlenk tube techniques. THF, ether, hexanes, benzene, toluene (Na−K alloy), CH_2Cl_2 (P_2O_5), and EtOH [$Mg(OEt)_2$] were treated with appropriate drying agents, distilled, and stored under argon. ^1H and ^{13}C NMR spectra were recorded on JEOL GX-270 (^1H NMR, 270 MHz; ^{13}C NMR, 67 MHz) and EX-400 (^1H NMR, 400 MHz; ^{13}C NMR, 100 MHz) spectrometers. Solvents for NMR measurements containing 0.5% TMS were dried over molecular sieves, degassed, distilled under reduced pressure, and stored under Ar. IR spectra (KBr pellets) and mass spectra (FD) were obtained on a JASCO FT/IR 5300 spectrometer and a Hitachi M-80 mass spectrometer, respectively. Complexes **1**,[8b] **1***,[8b] **2***,[8k] $Ru_3(CO)_{12}$,[23] $Fe_2(CO)_9$,[24] and $[Cp_2Fe]PF_6$[25] were prepared according to the published methods. ^{13}CO-enriched $Ru_3(CO)_{12}$ was prepared by heating a toluene suspension of $Ru_3(CO)_{12}$ under ^{13}CO (4 atm) for 3 days at 120 °C. Other chemicals were purchased and used as received. Chromatography was performed on alumina.

Reaction of 1 with $Ru_3(CO)_{12}$. A benzene solution (15 mL) of **1** (227 mg, 1.10 mmol) and $Ru_3(CO)_{12}$ (651 mg, 1.00 mmol) was refluxed for 1.5 h. After removal of the volatiles, the

(23) Bruce, M. I.; Jensen, C. M.; Jones, N. L. *Inorg. Synth.* **1990**, *28*, 216.
(24) King, R. B. *Organomet. Synth.* **1965**, *1*, 93.
(25) Sohn, Y. S.; Hendrickson, D. N.; Gray, H. B. *Inorg. Chem.* **1971**, *10*, 1559.

products were extracted with ether and passed through an alumina plug. Crystallization from ether−hexanes gave **3** (223 mg, 0.29 mmol, 29% yield). **3**. ^{1}H NMR ($CDCl_3$): δ_H −20.05 (1H, s, Ru−H), 3.90 (5H, s, Cp). ^{13}C NMR ($CDCl_3$): δ_C 79.7 (s, ≡C−Fe), 86.7 (d, J = 177 Hz, Cp), 174.1 (s, Ru−C≡), 190−194 (br, Ru−CO), 212.6 (s, Fe−CO). IR: 2084, 2036, 1986, 1978, 1963 cm^{-1}. Anal. Calcd for $C_{18}H_6O_{11}FeRu_3$: C, 28.55; H, 0.80. Found: C, 28.62; H, 0.83.

Reaction of 1* with $Ru_3(CO)_{12}$. A benzene solution (30 mL) of **1*** (0.58 g, 2.12 mmol) and $Ru_3(CO)_{12}$ (1.03 g, 1.61 mmol) was refluxed for 4 h. After removal of the volatiles, the resulting solid was washed with hexanes (10 mL × 3). Extraction with CH_2Cl_2 and filtration through a silica gel pad followed by crystallization from CH_2Cl_2−hexanes gave **3*** (992 mg, 1.20 mmol, 75% yield). **3***. ^{1}H NMR ($CDCl_3$): δ_H −19.56 (1H, s, Ru−H), 1.25 (15H, s, Cp*). ^{13}C NMR ($CDCl_3$): δ_C 9.5 (q, J = 128 Hz, $C_5\mathit{Me}_5$), 96.8 (s, ≡C−Fe), 97.5 (s, C_5Me_5), 168.1 (s, Ru−C≡), 215.1 (s, Fe−CO). IR: 2078, 2050, 2024, 2005, 1996, 1987, 1962 cm^{-1}. Anal. Calcd for $C_{23}H_{16}O_{11}FeRu_3$: C, 33.39; H, 1.95. Found: C, 33.19; H, 1.80.

Reaction of 2* with $Ru_3(CO)_{12}$. A benzene solution (40 mL) of **2*** (803 mg, 1.69 mmol) and $Ru_3(CO)_{12}$ (803 mg, 1.26 mmol) was refluxed for 9 h. After removal of the volatiles under reduced pressure, products were extracted with CH_2Cl_2 and passed through a Florisil plug. Concentration followed by cooling at −20 °C gave unreacted $Ru_3(CO)_{12}$ (177 mg). Further concentration of the filtrate followed by cooling at −20 °C gave **5*** (192 mg, 0.22 mmol, 25% yield based on the consumed $Ru_3(CO)_{12}$) as dark-purple crystals. Further separation of the filtrate by alumina column chromatography (eluted with 1:4 CH_2Cl_2−hexanes) afforded **6*** (82 mg, 0.05 mmol, 11% yield) as black crystals. **5***. ^{1}H NMR ($CDCl_3$): δ_H 1.55 (30H, s, Cp*). ^{13}C NMR ($CDCl_3$): δ_C 9.5 (q, J = 128 Hz, $C_5\mathit{Me}_5$), 98.0 (s, C_5Me_5), 177.2 (s, μ_4-C_2), 191.1, 196.4, 205.6 (Ru−CO), 217.8 (Fe−CO), 262.5 (μ-CO). IR: 2082, 2048, 1997, 1981, 1963, 1953, 1775 cm^{-1}. Anal. Calcd for $C_{32}H_{30}O_{10}Fe_2Ru_2$: C, 43.26; H, 3.40. Found: C, 43.50; H, 3.66. **6***. ^{1}H NMR (CD_2Cl_2): δ_H 1.61 (30H, s, Cp*). ^{13}C NMR (CD_2Cl_2 at 25 °C): δ_C 9.0 (q, J = 128 Hz, $C_5\mathit{Me}_5$), 98.7 (s, C_5Me_5), 190.1, 191.1, 194.2 (CO), 202.9, 208.4 (C_2), 210.7 (CO), 243.5 (μ-CO). ^{13}C NMR (CD_2Cl_2 at −80 °C): δ_C 9.4 ($C_5\mathit{Me}_5$), 98.6 (C_5Me_5), 190.5, 190.9, 191.4, 194.4, 197.2, 200.8 (CO), 203.2, 209.0 (C_2), 210.4 (CO), 244.5 (μ-CO). IR: 2076, 2057, 2016, 1836 cm^{-1}. Anal. Calcd for $C_{42}H_{32}O_{17}Cl_2Fe_2Ru_6$: C, 32.55; H, 2.00. Found: C, 32.78; H, 2.06.

Preparation of 5*. A mixture of **2*** (1.01 g, 2.05 mmol) and $Ru_3(CO)_{12}$ (1.06 g, 2.26 mmol) dissolved in benzene (60 mL) was refluxed for 6 h. After the mixture was left overnight at −30 °C, the frozen mixture was thawed and the supernatant solution was removed via a cannula. The residue was extracted with a CH_2Cl_2−hexane mixture and passed through a short alumina column (5 cm). After $Ru_3(CO)_{12}$ and Fp^*_2 were eluted with CH_2Cl_2−hexane, the product was eluted with ether. Evaporation of the ether solution gave **5*** (1.03 g, 1.20 mmol, 59% yield).

Preparation of 6*. A toluene solution (60 mL) of **2*** (312 mg, 0.60 mmol) and $Ru_3(CO)_{12}$ (372 mg, 0.58 mmol) was refluxed for 3.5 h. After removal of the volatiles under reduced pressure, the residue was subjected to alumina column chromatography and $Ru_3(CO)_{12}$ and Fp^*_2 were eluted with CH_2Cl_2−hexane (1:4). A purple-gray band eluted with CH_2Cl_2−hexane (1:3−1:2) was collected. Complex **6*** (0.12 g, 0.08 mmol, 26% yield) was obtained by evaporation of the solvent.

Reaction of 5* with $Ru_3(CO)_{12}$. A toluene solution (10 mL) of **5*** (35 mg, 0.05 mmol) and $Ru_3(CO)_{12}$ (32 mg, 0.02 mmol) was refluxed for 3 h. Removal of the volatiles under reduced pressure followed by silica gel TLC separation gave **3*** (17 mg, 0.02 mmol, 50% yield) and **6*** (6 mg, 0.004 mmol, 20% yield), which were characterized by IR and ^{1}H NMR. Other minor products could not be characterized.

Thermolysis of 3*. A toluene solution of **3*** (78 mg, 0.10 mmol) was refluxed for 11 h. Removal of the volatiles under reduced pressure followed by silica gel TLC separation gave **6*** (30 mg, 0.021 mmol, 42% yield based on consumed **3***) and **3*** (recovered, 40 mg, 0.05 mmol), which were characterized by IR and ^{1}H NMR. Other minor products could not be characterized.

Reaction of 3* with $Fe_2(CO)_9$. A THF solution (10 mL) of **3*** (96.0 mg, 0.112 mmol) and $Fe_2(CO)_9$ (81 mg, 0.22 mmol) was heated for 15 h at 65 °C. After removal of the volatiles, separation by column chromatography afforded Fp^*_2 (6.0 mg, 0.012 mmol), yellow compound **10*** (7.2 mg, 0.092 mmol, 8% yield based on consumed **3***), and **3*** (recovered, 35 mg, 0.041 mmol). **10***. ^{1}H NMR ($CDCl_3$): δ_H −20.1 (1H, s, Ru−H), 1.90 (15H, s, Cp*). ^{13}C NMR ($CDCl_3$): δ_C 10.1 (q, J = 128 Hz, $C_5\mathit{Me}_5$), 97.6 (s, C_5Me_5), 100.0 (s, ≡C−Fe), 182.8 (s, Ru−C≡), 213.8, 214.7 (s, Fe−CO). IR: 2085, 2057, 2021, 2005, 1992, 1965, 1943 cm^{-1}. Anal. Calcd for $C_{23}H_{16}O_{11}Fe_2Ru_2$: C, 35.32; H, 2.06. Found: C, 35.07; H, 2.06.

Protonation of 5*. (i) With CF_3SO_3H or HBF_4·OEt_2. To a CH_2Cl_2 solution of **5*** cooled in an ice bath was added CF_3SO_3H or HBF_4·OEt_2 (2 equiv), and the resulting mixture was stirred at ambient temperature. IR monitoring indicated a shift of the μ-CO vibration from 1783 cm^{-1} (**5***) to 1837 cm^{-1} (**11***). Attempted isolation of the product by addition of hexane gave [Fp*−CO]X. **11***. ^{1}H NMR data are in the text. IR (CH_2Cl_2): 2123, 2102, 2061, 2048, 2029, 1837 cm^{-1}.

(ii) With CF_3COOH. Reaction was carried out as described above. ^{1}H NMR data are in the text. IR (CH_2Cl_2): 2101, 2050, 2026, 1986, 1803 cm^{-1}.

Thermolysis of 3. A toluene solution (10 mL) of **3** (119 mg, 0.16 mmol) was refluxed for 3.5 h. After removal of the volatiles, products were separated by silica gel TLC eluted with 1:2 hexane−CH_2Cl_2. From the top brown band, black product **12** (23 mg, 0.018 mmol, 28% yield based on consumed **3**) was isolated, and from the next yellow band the starting compound **3** (0.031 mmol) was recovered. A trace amount of permetalated ethane **6** was isolated from a middle purple-red band. **6**. ^{1}H NMR ($CDCl_3$): δ_H 4.71 (10H, s, Cp). IR (KBr): 2082, 2063, 2022, 1856 cm^{-1}. FAB-MS: m/z 1373, 1373 − 28n (n = 1−17). An analytically pure sample could not be obtained despite several attempts. **12**. ^{1}H NMR (C_6D_6): δ_H 8.64 (1H, s, C_2H), 5.13 (5H, s, Cp). IR: 2071, 2005, 1962, 1824 cm^{-1}. Anal. Calcd for $C_{25}H_6O_{16}FeRu_6$: C, 24.52; H, 0.49. Found: C, 24.86; H, 0.95. FD-MS: m/z 1226 (the most intense peak).

Preparation of 13. To a THF solution (50 mL) of **3** (475 mmol, 0.628 mmol) was added an EtOH solution of KOH (53 mg, 0.94 mmol/12 mL) followed by an EtOH solution of PPh_4-Br (364 mg, 0.63 mmol/10 mL), while CO bubbling was maintained. After removal of the volatiles under reduced pressure, the residue was extracted with CH_2Cl_2 and passed through a Celite plug. Addition of ether gave orange solids, crystallization of which from acetone-ethanol afforded **13** as orange crystals (193 mg, 0.176 mmol, 28% yield). **13**. ^{1}H NMR (acetone-d_6): δ_H 8.05−7.84 (20H, m, PPh_4), 5.15 (5H, s, Cp). ^{13}C NMR (acetone-d_6): δ_C 215.0 (s, Fe−CO), 203.5 (s, Ru−CO), 187.0 (s, Ru−C≡), 136.4 (d, J_{CP} = 2 Hz, p-Ph), 135.7 (d, J_{CP} = 10 Hz, m-Ph), 131.4 (d, J_{CP} = 13 Hz, o-Ph), 119.1 (d, J_{CP} = 90 Hz, *ipso*-Ph), 88.2 (s, Cp), 74.3 (s, Fe-≡). IR: 2045, 2026, 1993, 1950, 1926 cm^{-1}. Anal. Calcd for $C_{40}H_{25}O_9PFeRu_3$: C, 46.21; H, 2.42. Found: C, 46.42; H, 2.46.

Oxidation of 11* with $[Cp_2Fe]PF_6$. A CH_2Cl_2 solution (15 mL) of **11*** (294 mg, 0.268 mmol) and $[Cp_2Fe]PF_6$ (89 mg, 0.269 mmol) was stirred for 3 h at ambient temperature. After removal of the volatiles, the residue was subjected to silica gel TLC separation (eluted with 1:1 ether−hexane). Products **6** and **15** were isolated from brown and dark-red bands, respectively. Recrystallization gave **6** (43 mg, 0.031 mmol, 23% yield; from CH_2Cl_2−hexane) and **15** (23 mg, 0.018 mmol, 13% yield; from CH_2Cl_2−ether) as black thin plates and black crystals, respectively. **15**. ^{1}H NMR ($CDCl_3$): δ_H 4.98 (5H, s, Cp). IR: 2064, 2018, 1986, 1875 cm^{-1}. Anal. Calcd for $C_{31}H_{10}O_{17}Fe_2Ru_5$: C, 29.28; H, 0.79. Found: C, 29.56; H, 1.06.

Table 6. Crystallographic Data

	complex[a]			
	3	**5***	**6*·CH_2Cl_2**[d]	**10***
formula	$C_{18}H_6O_{11}FeRu_3$	$C_{32}H_{30}O_{10}Fe_2Ru_2$	$C_{42}H_{32}O_{17}Cl_2Fe_2Ru_6$	$C_{23}H_{16}O_{11}FeRu_3$
fw	757.3	888.42	1597.72	782.2
diffractometer	AFC5S	AFC5R	R-AXIS IV	AFC5R
temp (°C)	25	25	−60	25
cryst syst	orthorhombic	monoclinic	monoclinic	monoclinic
space group	*pbca*	*C*2/*c*	*C*2/*c*	$P2_1/n$
a/Å	15.166(2)	14.124(6)	19.545(5)	17.857(4)
b/Å	21.445(4)	11.537(5)	20.928(2)	10.156(1)
c/Å	14.025(2)	20.142(5)	23.886(4)	17.162(3)
β/deg		93.23(4)	96.102(4)	116.81(1)
V/Å^3	4561(2)	3277(4)	9714(2)	2777(1)
Z	8	4	8	4
d_{calcd}/g cm^{-3}	2.21	1.80	2.19	1.87
μ/cm^{-1}	25.9	18.1	25.7	21.4
2θ/deg	55	50	55	55
no. data collected	5818	6177	10 083	6963
no. data with $I > 3\,\sigma(I)$	2582	2668	8719[e]	5338
no. params refined	298	208	632	343
R[b]	0.053	0.059	0.055[f]	0.053
R_w[c]	0.040	0.050	0.173[g]	0.073

	complex[a]		
	12·CH_2Cl_2	**13**	**15**·$(H_2O)_{2/3}$
formula	$C_{26}H_8O_{16}Cl_2FeRu_6$	$C_{42}H_{25}O_{11}PFeRu_3$	$C_{31.67}H_{11.33}O_{17}Fe_2Ru_5$
fw	1309.5	1095.7	1283.5
diffractometer	AFC5R	AFC5R	AFC5R
temp (°C)	25	25	25
cryst syst	monoclinic	monoclinic	monoclinic
space group	$P2_1/c$	$P2_1/n$	*C*2/*c*
a/Å	11.848(5)	10.450(3)	42.215(5)
b/Å	10.812(5)	12.997(7)	15.776(5)
c/Å	27.739(4)	30.117(10)	16.842(4)
β/deg	99.11(2)	99.10(3)	100.06(2)
V/Å^3	3508(4)	4039(3)	11044(5)
Z	4	4	12
d_{calcd}/g cm^{-3}	2.48	1.80	2.32
μ/cm^{-1}	30.9	15.5	28.4
max 2θ/deg	55	50	50
no. data collected	8880	7894	10 261
no. data with $I > 3\,\sigma(I)$	5250	4173	6260
no. params refined	464	523	754
R[b]	0.035	0.042	0.052
R_w[c]	0.039	0.030	0.047

[a] Refined with teXsan[26] unless otherwise stated. [b] $R = [\sum||F_o| - |F_c||]/\sum|F_o|$. [c] $R_w = [\sum\{w(|F_o| - |F_c|)^2\}/\sum wF_o^2]^{0.5}$; $w = 1/\sigma^2(F_o^2)$. [d] Refined with SHELXS97.[32b] [e] Number of data with $I > 2\,\sigma(I)$. [f] R1 $= [\sum||F_o| - |F_c||]/\sum|F_o|$ (for data with $I > 2\,\sigma(I)$). [g] wR2 $= [\sum\{w(F_o^2 - F_c^2)\}^2/\sum\{w(F_o^2)^2\}]^{0.5}$; $w = 1/[\sigma^2(F_o^2) + (0.1000P)^2]$ where $P = [2F_c^2 + \max(F_o^2,0)]/3$ (for all data).

Experimental Procedure for X-ray Crystallography. (i) For 3, 5*, 10*, 12, 13, and 15. Suitable single crystals were mounted on glass fibers. Diffraction measurements were made on Rigaku AFC5S (**3**) and AFC5R (**5***, **10***, **12**, **13**, and **15**) automated four-circle diffractometers at 25 °C by using graphite-monochromated Mo Kα radiation (λ = 0.710 69 Å). The unit cells were determined and refined by a least-squares method using 20 independent reflections (2$\theta \approx$ 20°). Data were collected with ω−2θ (**3**, **5***, **10***) and ω scan techniques (**12**, **13**, **15**). If $\sigma(F)/F$ was more than 0.1, a scan was repeated up to three times and the results were added to the first scan. Three standard reflections were monitored every 100 (**3**) and 150 measurements (the others). The data processing (data collection) was performed on FACOM A-70 (**3**) and Microvax II computers (the others). In the reduction of data, Lorentz and polarization corrections were made. An empirical absorption correction (Ψ scan) was made.

Crystallographic data and the results of refinements are summarized in Table 6. Structure analysis was performed on a Microvax II computer by using the teXsan structure solving program obtained from the Rigaku Corp., Tokyo, Japan.[26] Neutral scattering factors were obtained from the standard source.[27] The structures were solved by a combination of direct methods (MITHRIL90[28] and SAPI91[29]) and DIRDIF.[30] Unless otherwise stated, non-hydrogen atoms were refined with anisotropic thermal parameters and hydrogen atoms were fixed at the calculated positions (C−H = 0.95 Å) and were not

(26) *teXsan, Crystal Structure Analysis Package*; Rigaku Corp.: Tokyo, Japan, 1985, 1992, and 1999.

(27) *International Tables for X-Ray Crystallography*; Kynoch Press: Birmingham, 1975; Vol. 4.

(28) Gilmore, C. J. *MITHRIL, an integrated direct methods computer program*; University of Glasgow: Glasgow, U.K., 1990.

(29) Fan, H.-F. *Structure Analysis Programs with Intelligent Control*: Rigaku Corp.: Tokyo, Japan, 1991.

(30) Beurskens, P. T.; Admiraal, G.; Beurskens, G.; Bosman, W. P.; Garcia-Granda, S.; Gould, R. O.; Smits, J. M. M.; Smykalla, C. *The DIRDIF program system, Technical Report of the Crystallography Laboratory*; University of Nijmegen: Nijmegen, The Netherlands, 1992.

refined. The C_2H atom in **12** was refined isotropically, and the bridging hydrogen atoms of **3** and **10*** were not included in the refinements.

(ii) For 6*. Diffraction measurements were made on a Rigaku RAXIS IV imaging plate area detector with Mo Kα radiation ($\lambda = 0.710\ 69$ Å). All the data collections were carried out at −60 °C. Indexing was performed from these oscillation images, which were exposed for 4 min. The crystal-to-detector distance was 110 mm. Data collection parameters were as follows: detector swing angle, 5°; number of oscillation images, 23; exposed time, 50 min. Readout was performed with a pixel size of 100 μm × 100 μm.

Crystallographic data and the results of refinements are summarized in Table 4. The structural analysis was performed on an IRIS O2 computer using the teXsan structure solving program obtained from the Rigaku Corp., Tokyo, Japan. Neutral scattering factors were obtained from the standard source.[27] In the reduction of data, Lorentz and polarization corrections were made. An absorption correction was also made.[31]

The structures were solved by a combination of direct methods (SHELXS 86)[32] and DIRDIF[28] and refined with the SHELXS97 least-squares refinement program.[32] Non-hydrogen atoms were refined with anisotropic thermal parameters. The methyl hydrogen atoms were refined using the riding models, and the other hydrogen atoms were fixed at the calculated positions (C−H = 0.95 Å) and not refined.

Acknowledgment. We are grateful to the Yamada Science Foundation for financial support of this research. We thank JEOL, Ltd. for the measurement of the FAB-MS spectrum of **6**.

Supporting Information Available: Experimental details for X-ray crystallography and crystallographic results. This material is available free of charge via the Internet at http://pubs.acs.org.

OM001009C

(31) Higashi, T. *Shape, Program To Obtain Crystal Shape Using CCD Camera*; Rigaku Corp.: Tokyo, Japan, 1999.

(32) (a) Sheldrick, G. M. *SHELXS-86: Program for crystal structure determination*; University of Göttingen: Göttingen, Germany, 1986. (b) Sheldrick, G. M. *SHELXL-97: Program for crystal structure refinement*; University of Göttingen: Göttingen, Germany, 1997.